## 2022 ANNUAL REPORT





Nuclear Science User Facilities 995 MK Simpson Blvd. Idaho Falls, ID 83401-3553 nsuf.inl.gov

On the front cover:

The Long Beamline Building construction at Argonne National Laboratory (credit, Argonne National Laboratory).

#### Disclaimer

This information was prepared as an account of work sponsored by an agency of the U.S. Government. Neither the U.S. Government nor any agency thereof, nor any of their employees, makes any warranty, expressed or implied, or assumes any legal liability or responsibility for the accuracy, completeness, or usefulness, of any information, apparatus, product, or process disclosed, or represents that its use would not infringe privately owned rights. References herein to any specific commercial product, process, or service by trade name, trade mark, manufacturer, or otherwise, does not necessarily constitute or imply its endorsement, recommendation, or favoring by the U.S. Government or any agency thereof. The views and opinions of authors expressed herein do not necessarily state or reflect those of the U.S. Government or any agency thereof.

Editors: Tiera Cate, Rachel Hansen, Rebecca Jones, Jeffrey Pinkham, Barney Hadden

Writers: Tiera Cate, Cory Hatch

Graphic Designers: Vanessa Godfrey, Kristyn St. Clair

### TABLE OF CONTENTS

Nuclear Science User Facilities	
Our NSUF Program Office Team	6
From the Departing NSUF Director	3
From the Incoming NSUF Director	10
NSUF Overview	
NSUF By the Numbers	12
NSUF Across the Nation	14
Highlights from the Year	16
Capability Updates	20
High-Performance Computing	22
Nuclear Fuels and Materials Library	30
Activated Materials Laboratory	34
Getting to Know the NSUF Team	40
NSUF Awarded Projects	
Awarded Projects	ΔΔ

# CONTENTS

NSUF Awarded Projects	
Technical Reports	2
Short Communications	4
<ul> <li>ChemiSTEM Characterization of Bulk Heavy         Ion-Irradiated Complex Concentrated Alloys</li></ul>	C 4
Complex Alloys under Dual-Beam Heavy-Ion Irradiation9	C
Resources  NSUF List of Acronyms9	6



### OUR NSUF PROGRAM OFFICE **TEAM**



J. Rory Kennedy, Ph.D. **Departing Director** (208) 526-5522 rory.kennedy@inl.gov



Brenden Heidrich, Ph.D. Incoming Director and **Chief Irradiation Scientist** (208) 526-8117 brenden.heidrich@inl.gov

**Collin Knight Deputy Director** (208) 533-7707 collin.knight@inl.gov



**Jeff Benson** Rapid Turnaround **Experiment Administrator** (208) 526-3841 jeff.benson@inl.gov



**Matt Anderson** High-Performance Computing Manager (208) 526-4104 matthew.anderson2@inl.gov



**Leigh Astle** Experiment Manager (208) 526-1154 leigh.astle@inl.gov



**Tiera Cate** Communications Liaison (208) 526-4828 tiera.cate@inl.gov



(208) 526-3527 matthew.arrowood@inl.gov

Megan Broadhead Planning and Financial

Controls Specialist (208) 526-7219 megan.broadhead@inl.gov

**Lindy Bean** 

(208) 526-4662 lindy.bean@inl.gov

**Kelly Cunningham** 

Materials Library Coordinator

kelly.cunningham@inl.gov

**Matthew Arrowood** 

Experiment Manager

Nuclear Fuels and

(208) 526-2369

Consolidated Innovative

Nuclear Research Administrator





**Michael Heighes Mechanical Properties** Technical Lead (208) 526-1785 michael.heighes@inl.gov

Travis Howell Experiment Manager (208) 526-3817 travis.howell@inl.gov



**Keith Jewell, Ph.D.** *Technical Lead* (208) 526-3944 *james.jewell@inl.gov* 

William McClung Project Scheduler william.mcclung@inl.gov





Simon Pimblott, D. Phil. Chief Post Irradiation Scientist (208) 526-7499 simon.pimblott@inl.gov

Aaron Russell Experiment Manager (208) 526-6984 aaron.russell@inl.gov





**Trevor Smuin** *Experiment Manager*(208) 526-5236
trevor.smuin@inl.gov

Rongjie Song Technical Lead (208) 526-5117 rongjie.song@inl.gov





Renae Tripp Administrative Assistant (208) 526-6918 renae.tripp@inl.gov

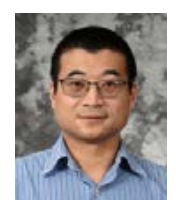
**Dain White** Technical Lead Software Engineer (208) 533-8210 dain.white@inl.gov





Eric Whiting
Director of High
Performance Computing
(208) 526-1433
eric.whiting@inl.gov

Peng Xu, Ph.D. Industry Program Lead (208) 533-8163 peng.xu@inl.gov





Alina Zackrone
Post Irradiation Examination
Experiment Manager
(208) 526-6086
alina.zackrone@inl.gov

# DEPARTING DIRECTOR



J. Rory Kennedy, Ph.D.
Departing Director
(208) 526-5522
rory.kennedy@inl.gov

I thought the FY-21 Annual Report might contain my last "From the Director" message, but since I was still the director throughout 2022, I am obliged to punish you with one final contribution. As I mentioned last year, my goal was to see our budget restored to at least pre-2020 levels so that the NSUF could once again achieve its earlier levels of cutting-edge and innovative research. A slight increase in our budget from 2021, coupled with a small decrease in congressional mandates, allowed for a recovery of about 25% of the effective budget lost in 2020. In addition, these changes to the budget enabled us to continue our funding toward solicitations, database updates and other efforts. All in all, we had another successful year thanks to the efforts of the NSUF staff, the Department of Energy Office of Nuclear Energy, our partners and our engaged users.

We saw remarkable proposals from our users and made 34 awards, including 30 Rapid Turnaround Experiments and four Consolidated Innovative Nuclear Research projects. The NSUF allocated about \$13 million to

these projects, including direct investment, supporting activities, and establishing full-life-cycle management of all our projects. Typically, the NSUF manages between 100 and 130 projects at a time. The NSUF senior leadership experienced some significant changes in 2022 and going into 2023, which started with losing Deputy Director Dan Ogden to retirement midyear. Thanks, Dan, for all you did for the program. It was fun working with you. Collin Knight, who has been with the program since the beginning as our postirradiation examination coordinating manager, succeeded Dan. Of course, that change left a hole in our post-irradiation examination coordination, and Alina Zackrone stepped in to replace Collin. So, who will replace me? The NSUF is fortunate that our Chief Irradiation Scientist Brenden Heidrich agreed to take the reins. He has been with the NSUF since 2014 and will do an exceptional job leading the program. Now Brenden will need to find a chief scientist to replace himself. We continued to add exceptional talent with additional experiment managers, Leigh Astle and Trevor Smuin, and our new planning and



financial controls specialist, Megan Broadhead. I can say with the highest confidence that the NSUF is in good hands moving forward.

With everyone's contributions, we completed 10 Consolidated Innovative Nuclear Research projects, 24 of 29 Rapid Turnaround Experiments, and six neutron irradiations in five reactors. In addition, our Nuclear Fuels and Materials Library expanded and added over 700 samples. The productivity from NSUF users was once again impressive in FY-22, producing 128 peer-reviewed publications. To date, NSUFsupported research has produced over 725 peer-reviewed journal publications, generating almost 7,700 citations that result in a cumulative h-index of 40 (Clarivate Web of Science) as of Sept. 30, 2022.

With travel restrictions lifted, we returned to conferences and meetings, and visited potential partner facilities. Some travel where we exhibited the NSUF included the American Chemical Society Fall Meeting, the TopFuel Light

Water Reactor Fuel Performance Conference, the Nuclear Materials Conference, the American Nuclear Society Annual Meeting and the Winter Meeting and Technology Expo (organized and chaired sessions at both), and the Materials Research Society Fall Meeting.

Internationally, we continued our leadership role in the U.S. and U.K. Civil Nuclear Energy Research and Development Action Plan's Enabling Technology Working Group and continued to push forward on the Disc Irradiation for Separate Effects Testing, or DISECT, project with the Belgian Nuclear Research Centre. The NSUF also had several interactions with the new OFFERR (eurOpean platForm For accEssing nucleaR R&d facilities) project out of the European Commission Euratom framework, with an objective to build a European user facility network. The NSUF provided a range of input and was invited to present at the project's kickoff meeting. Many of the features and aspects of OFFERR are similar to the NSUF, which we take as an indication of our success and influence.

I expressed my sincerest thanks last year, and all I can do here is mostly repeat what I stated since my gratitude remains the same. I thank everyone I have had the pleasure of working and interacting with over the nine years of my tenure, including all the NSUF staff members (I'll think of you every time I barbeque some ribs), all the staff and instrument scientists at INL and the partner facilities, members of the Science Review Board, the Users Organization, the DOE Office of Nuclear Energy staff for their unrelenting support (especially Mike Worley who was with me from the start), and, of course, our users. It has been an exceptional experience, and I believe we have made remarkable contributions to the science and engineering needed to advance nuclear energy. The future is looking very exciting, and the NSUF will be a major part of it.

J. Ky Ly

J. Rory Kennedy, Ph.D.

## INCOMING DIRECTOR



Brenden Heidrich, Ph.D. Incoming Director and Chief Irradiation Scientist (208) 526-8117 brenden.heidrich@inl.gov

For the last eight years, I have worked with the Nuclear Science User Facilities as the chief irradiation scientist. Throughout this time, I have gotten to know many incredible people who help the NSUF program meet its goals, including the program staff at INL, the federal contingent at the Department of Energy, our partner facilities, and, of course, our user community. As the NSUF faces challenges and opportunities ahead, I intend to build upon the legacy of the last 15 years of excellence and adopt new technologies to support our sponsor and users well into the future.

I started with NSUF in 2014, building a database of nuclear energy research and development capabilities that developed into an online toolset of capabilities for our users. More recently, I managed INL's Post-Irradiation and Irradiation departments in the Nuclear Fuels and Materials division, supporting experiments for NSUF and other research and development programs at the Advanced Test Reactor and Transient Reactor Test Facility at

INL and the other reactors in the NSUF partnership. Before coming to INL, I was the assistant director at Pennsylvania State University's Radiation Science and Engineering Center. Additionally, I served in the U.S. Navy as a nuclear reactor operator on the USS Enterprise. I taught nuclear physics and nuclear security and safeguards.

I feel fortunate to have been part of the NSUF these past years and am honored to lead the organization. Over the years, I have been motivated by the passion and commitment of our staff, partners, users, and program office. My passion is helping others solve their problems, as a professor, scientist, manager and now as the NSUF director.

I want to thank Rory Kennedy, who has served as the director for the NSUF over the last nine years. His dedication and commitment to the program have been inspiring. As the next leader, I promise that I will continually strive to advance nuclear energy technology and meet our nation's energy goals.



Over the next few months, I will work with the NSUF user community, our NSUF partner organizations, nuclear engineering and materials university faculty members, and the Department of Energy Office of Nuclear Energy to help set the direction for future NSUF operations and investments. One area I will focus on will be reaching out to underrepresented and underserved groups of researchers. Working at Idaho National Laboratory and leading the NSUF is the pinnacle of my career. I want to ensure that everyone has the same chance to positively impact our nation's energy future.

I look forward to continuing to serve the NSUF mission in this manner. I will be accountable to our research community and transparent in my decision-making. I promise to roll up my sleeves and do the hard work.

There is much work to be done. I'm grateful to work with this dedicated community and thank you all for your support.

SHE

Brenden Heidrich, Ph.D. PE

# NSUF BY THE NUMBERS

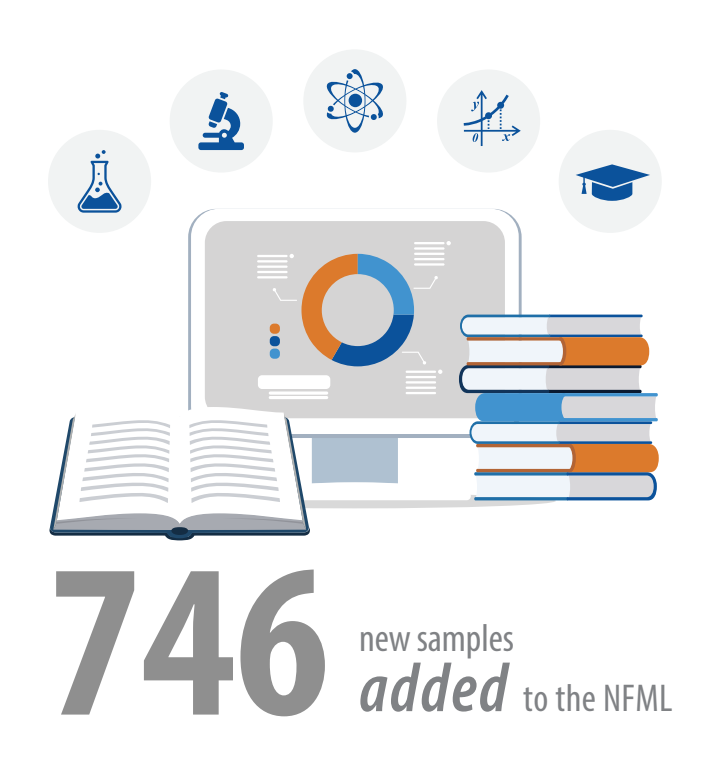
Note: Numbers for FY-22 only.

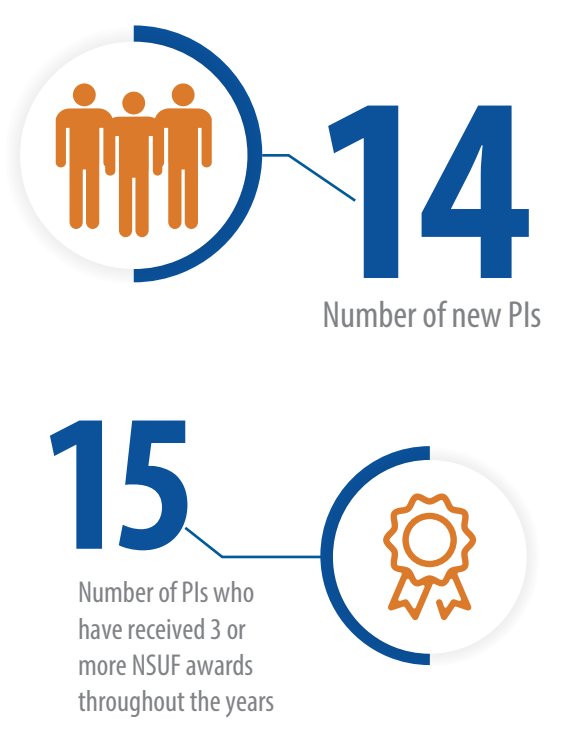


20 3% 0% **32**% **65%** user Industry International National Universities institutions Organizations Laboratories received awards in FY-22

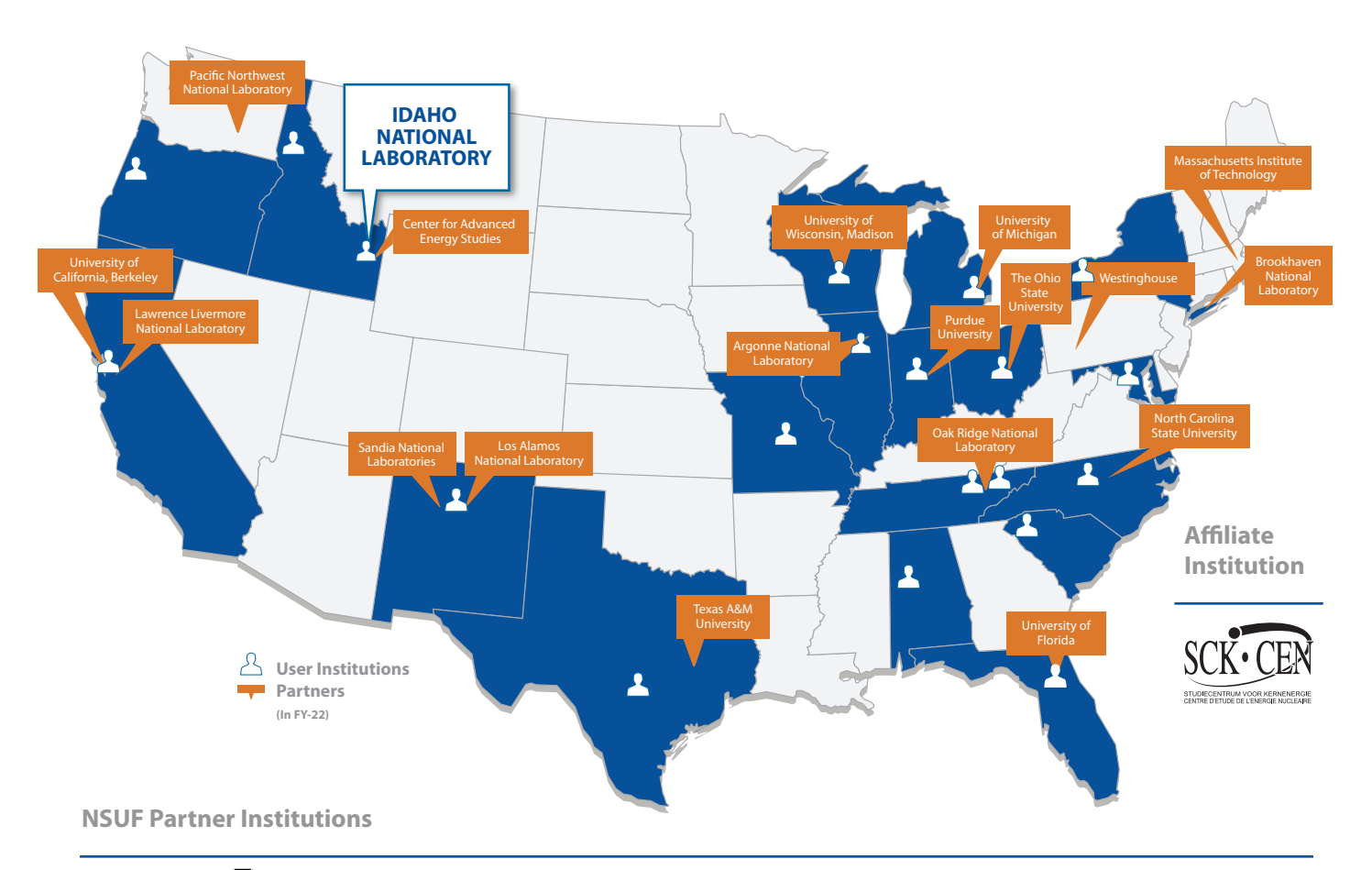
# 37) PERCENT

of projects involve a graduate student, either as a PI or a collaborator





# NSUF ACROSS THE NATION





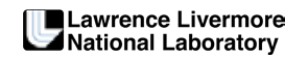








































#### **NSUF User Institutions (FY-22)**

Alabama

University of Alabama

Michigan

University of Michigan

**South Carolina** 

Clemson University

California

Kairos Power, LLC

Missouri

Missouri Science and Technology

**Tennessee** 

Oak Ridge National Laboratory University of Tennessee

Florida

University of Florida

**New Mexico** 

Los Alamos National Laboratory

Texas

University of Texas-San Antonio

Idaho

Idaho National Laboratory University of Idaho

**New York** 

University at Buffalo

Wisconsin

University of Wisconsin-Madison

Illinois

Argonne National Laboratory

**North Carolina** 

North Carolina State University

Indiana **Purdue University**  Oregon

**Oregon State University** 

Maryland

**Nuclear Regulatory Commission** 

Ohio

The Ohio State University

# FROM THE YEAR

This year, some of the NSUF's successes have included completing all eight major milestones on schedule, adding nearly 800 samples to the Nuclear Fuels and Materials Library, expanding capabilities, and more. However, capabilities are not the only successes that matter. The Department of Energy Office of Nuclear Energy's support enables the program to continue its mission Not only is it critical for DOE-NE to be aware of the program's output and activities, but it's also essential to have outside perspectives. Since the COVID-19 pandemic hit, this was the first year that the NSUF representatives hosted in-person meetings, traveled to conferences, and widely spoke about the successful projects and administration behind the program.

### Integrating with the research community: Conferences and meetings

The NSUF promotes, coordinates and executes research on behalf of DOE-NE, and it is critical that the program participates in opportunities to integrate with the research community. Meetings and conferences allow researchers to share their groundbreaking research with a broader audience and serve as avenues for collaboration, networking, and growth.

A central part of NSUF outreach is sending program representatives to trade and research society meetings that have strong nuclear fuel and materials connections. These meetings and conferences provide opportunities for the NSUF to interact with thousands of attendees, which include government, academic, and industry representatives. This outreach raises awareness to new

researchers and reconnects those currently participating in the NSUF program.

**NSUF Director Rory Kennedy** organized and chaired sessions at this year's American Nuclear Society winter and annual meetings. These were great opportunities to update attendees on the organization's contributions to advanced nuclear research. Highlighting the impactful work that the organization makes possible is critical to the NSUF's continued success. The NSUF also participated in the American Chemical Society's Fall Meeting, the TopFuel Light Water Reactor Fuel Performance Conference, the Nuclear Materials Conference, and the Materials Research Society Fall Meeting.



NSUF booth at the American Chemical Society meeting.



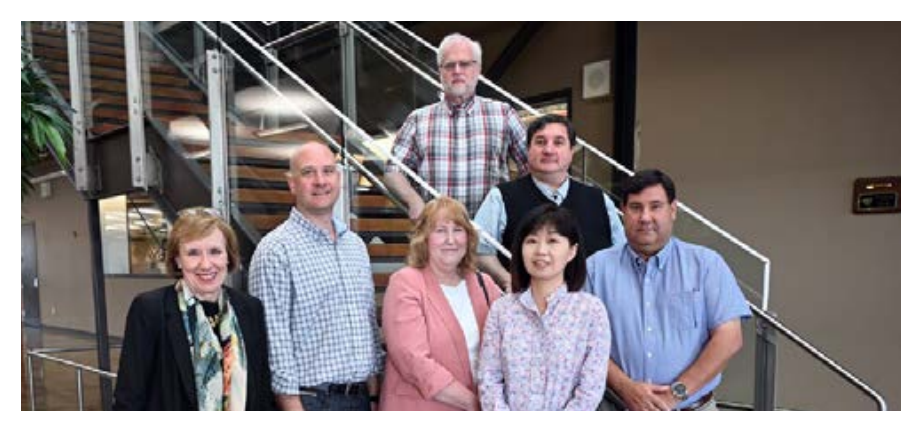
#### **Enhancing nuclear energy research: The Science Review Board**

Experts from industry, national laboratories and universities comprise the NSUF Science Review Board, which meets to examine the activities and output of the NSUF and provide fresh perspectives. Last held in 2018, the board reconvened in August 2022 at the Center for Advanced Energy Studies for a three-day meeting with NSUF, Idaho National Laboratory staff members and users. The board evaluates administration, research avenues and output, noting any recommendations that may fortify the program. To showcase their work, researchers presented results

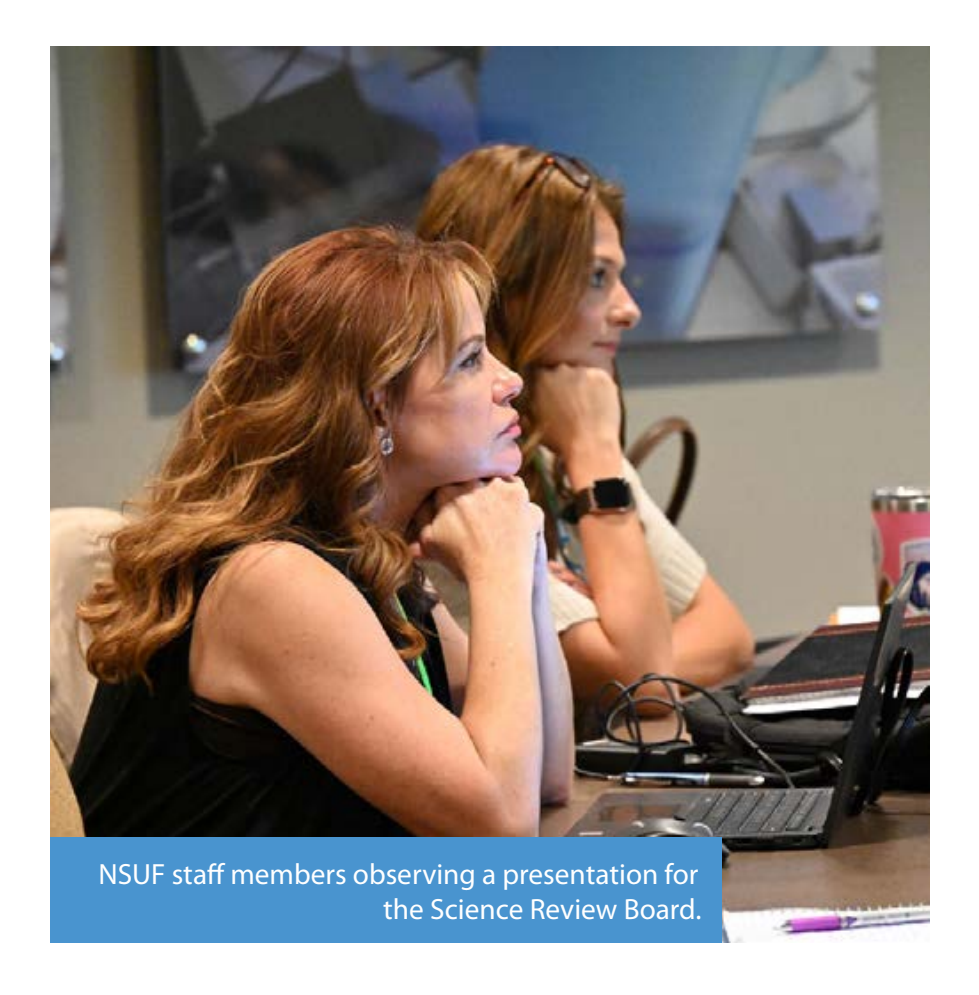
enabled by Rapid Turnaround Experiments or Consolidated Innovative Nuclear Research awards.

INL staff members updated the board on the Nuclear Science and

Technology directorate, provided a summary of the Advanced Test Reactor's core internals changeout, and outlined capabilities at the Materials and Fuels Complex.



The members of the Science Review Board.





Jeff Benson, RTE administrator, presenting to the Science Review Board.

Finally, the NSUF program office provided a status update on the industry engagement program, highperformance computing capabilities, the Nuclear Fuels and Materials Library, and other administrative processes that enable the program to conduct research. After presentations, the board develops a report that evaluates the NSUF's scientific output and may suggest ideas for improvement. Comments provided in the report are valuable in strengthening the NSUF program, creating a better user experience, and advancing DOE-NE's mission.

Members of the board are experts from a variety of backgrounds and locations. Board members include Sean McDeavitt from Texas A&M University, Jake Ballard from Naval Nuclear Laboratory, Lynne Ecker from TerraPower, Gabriel Meric from Kairos Power (chair of the users organization), Vincenzo Rondinella from European Commission's Joint Research Centre Karlsruhe Laboratory, David Senor from Pacific Northwest National Laboratory, Grace Burke from Oak Ridge National Laboratory, Meimei Li from Argonne National Laboratory, and Simerjeet Gill from Brookhaven National Laboratory.

Perhaps the most vital aspect of the Science Review Board is the outcome — the improvements made over the years that contribute to the continuation of meaningful, reliable, and affordable nuclear energy research.



#### Showcasing accomplishments: The annual program review

Every year, the NSUF meets with DOE-NE counterparts to illustrate accomplishments throughout the year. DOE-NE federal program managers, national technical directors and other interested parties were encouraged to attend this year's review for information on the NSUF and its supported work. This two-day meeting was mainly held in person, alongside invited virtual presentations.

Attendees heard from incoming DOE-NE NSUF Program Manager Christopher Barr, and applauded as he, alongside Alice Caponiti, presented Rory Kennedy with an award acknowledging his time serving as the NSUF director. The program review included informational presentations by the NSUF program office, technical lectures from selected NSUF

supported research projects, updates from instrument scientists and technical leads, and more.

Sharing updates and success in this way is critical in acknowledging the program's success and enabling the NSUF to support DOE-NE's mission.

# UPDATES

#### Propelling CAES into the future: New scanning transmission electron microscope



CAES scanning transmission electron microscope and a 3D metal printer ribbon cutting.

The Center for Advanced Energy Studies (CAES) held a ribbon-cutting ceremony in late 2022 to celebrate the installation of equipment that significantly enhances the advanced materials research capabilities at the CAES facility.

As Idaho National Laboratory's latest investment in CAES, the new scanning transmission electron microscope (STEM) provides ultrahigh resolution to characterize structure and energy. It brings CAES the highest resolution imaging and spectroscopic capabilities nationwide for nuclear science postirradiation examination.

The new equipment supports partnerships with academia, industry, federal agencies, and national laboratories through the Nuclear Science User Facilities network.

"I look forward to seeing how this new equipment, along with the laboratories they are in, can help propel CAES into the future," CAES Director Philip Reppert said.

## THERMOFISHER SPECTRA 300 SCANNING TRANSMISSION ELECTRON MICROSCOPE

- Monochromated, probe- and image-corrected
- 30 to 300 kV HT
- Single-electron-sensitive STEM detection (equipped with Panther, a new detector geometry offers access to advanced STEM imaging capability combined with the sensitivity and detectability to measure single electrons)
- Integrated differential phase contrast (iDPC) imaging for studying magnetic and electrical properties and optimized Z-contrast imaging from hydrogen to uranium
- Fully automated, single-click access to the highest-resolution STEM (<50 pm) and energyresolution EELS (<30 meV); drift corrected frame integration (DCFI)
- For magnetic property studies, field-free imaging in TEM Lorentz mode with 2 nm resolution
- Super-X 4 detector EDS system (≤136 eV for Mn-Kα and ten kcps (output)); Gatan Ultrafast EELS/ DualEELS
- Electron microscope pixel array detector (EMPAD) – 4D STEM
- Tilt range ±40 degrees for analytical double tilt holder; ±75 degrees for tomography holder





Top: Researchers Kaustubh Bawane, Yaqiao Wu and Ching-Heng Shiau working with the new Scanning Transmission Electron Microscope in the Center for Advanced Energy Studies. Bottom: An aerial view of the Center for Advanced Energy Studies in Idaho Falls, Idaho.

- Gatan Continuum Ultrafast
   DualEELS can achieve an energy
   resolution between <0.025 eV and
   <p>1 eV and record two energy ranges
   simultaneously
- Supports simultaneous EDS and EELS data acquisition

# COMPUTING



INL's supercomputers are one of the Nuclear Science User Facilities' 49 partner facilities and its only supercomputers.

From atoms to earthquakes to Mars: high-performance computing a swiss army knife for modeling and simulation

By Cory Hatch, INL Communications

Researchers solving today's most important and complex energy challenges can't always conduct real-world experiments.

This is especially true for nuclear energy research. Considerations such as cost, safety and limited resources can often make laboratory tests impractical. In some cases, the facility or capability necessary to conduct a proper experiment doesn't exist.

At Idaho National Laboratory, computational scientists use INL's supercomputers to perform "virtual experiments" to accomplish research that couldn't be done by conventional means. While supercomputing can't replace traditional experiments, it is an essential component of all modern scientific discoveries and advancements.

"Science is like a three-leg stool," said Eric Whiting, director of Advanced Scientific Computing at INL. "One leg is theory, one is experiment, and the third is modeling and simulation. You cannot have modern scientific achievements without modeling and simulation."



#### **HIGH DEMAND RESOURCES**

INL's High-Performance Computing program has been in high demand for years. From INL's first supercomputer in 1993 to the addition of the Sawtooth supercomputer in 2020, the demand for high-performance computing has only increased.

Sawtooth and INL's other supercomputers, Lemhi and Hoodoo, are flexible enough to tackle a wide range of modeling and simulation challenges and are especially suitable for dynamic and adaptive applications, like those used in nuclear energy research. INL's supercomputers are one of the Nuclear Science User Facilities' 49 partner facilities and its only supercomputers.

Whether it's exploring the effects of radiation on nuclear fuel or designing nuclear-powered rockets for a trip to Mars, INL's High-Performance Computing center is the swiss army knife of advanced computing.



### THE POWER OF 100,000 LAPTOPS

On a recent tour of the Collaborative Computing Center, Eric Whiting led the way through the rows of Sawtooth processors. Each row looked like dozens of tall black refrigerators standing side by side. The room hummed with the pumping of thousands of gallons of water needed to keep Sawtooth cool.

Sawtooth is INL's newest supercomputer, consisting of 2079 compute nodes each of which has 48 cores and 192 GB of memory.

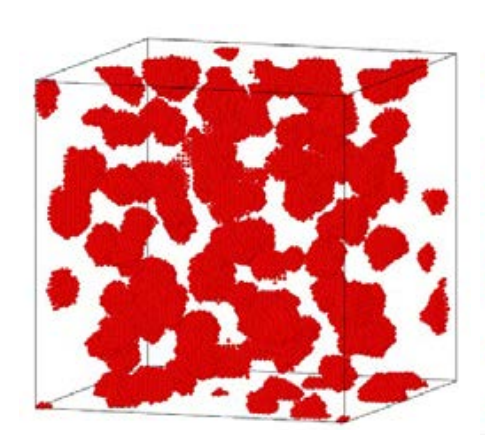
Sawtooth contains the computing power of about 100,000 processors all dedicated to very large, high-fidelity problems, which means orders of magnitude more processing power and memory when compared to a traditional laptop computer. All that computing power allows researchers from around the world to run dozens of complex simulations at the same time. "If your program is designed right, it runs thousands of times faster than the best-case scenario on your desktop," Whiting said.

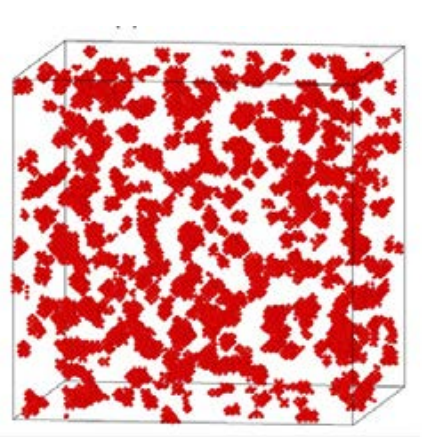
Some of these simulations — modeling the performance of fuel inside an advanced reactor core, for instance — require the computer to solve millions or billions of unknowns repeatedly.

"If you have a multidimensional problem in space, and then you add time to it, it greatly adds to the size of the problem," said Cody Permann, a computer scientist who oversees one of the laboratory's modeling and simulation capabilities. Modeling and simulation started decades ago by solving simplified problems in one or two dimensions. Modern supercomputers, like INL's Sawtooth, significantly increased the accuracy of these simulations, bringing them closer to reality.

To solve these complicated problems, researchers break down each simulation into thousands upon thousands of smaller units, each impacting the units surrounding it. The more units, the more detailed the simulation, and the more powerful the computer needed to run it.

This visualization shows how an Fe-20Cr alloy changes when exposed to 773 K (931° F) between 41 hours (left) and 1000 hours (right). For clarity of visualization, only Cr atoms are shown.





### THE ATOMIC EFFECTS OF RADIATION ON MATERIALS

For Chao Jiang, a distinguished staff scientist at INL, a highly detailed simulation means peering down to the level of individual atoms.

Jiang's simulations, funded by the Department of Energy Nuclear **Energy Advanced Modeling and** Simulation the Basic Energy Sciences programs. and the Basic Energy Sciences program, help nuclear scientists understand the behavior of materials when their atoms are knocked around by neutrons in a reactor core. These displaced atoms will create radiation damage in the material, like point defects and defect clusters, changing the material's microstructure and, therefore, its physical and mechanical characteristics. These changes in microstructure can reduce the strength of the materials and limit the reactor's lifetime. Understanding these changes helps scientists design better and even safer reactors.

This visualization shows how an Fe-20Cr alloy's changes when exposed to 773 K (931° F) between 41 hours (left) and 1000 hours (right). For clarity of visualization, only Cr atoms are shown.

"The work we are doing is extremely challenging," Jiang said. "They are computer-hungry projects. We are big users of the high-performance computers."

Understanding the radiation damage in materials is difficult. This change involves physical processes that occur across vastly different time and length scales. "When the high energy neutrons hit the material," Jiang said, "it will locally melt the material."

Heating and cooling inside an operating reactor takes place in picoseconds, or one trillionth of a second. During this heating and cooling, the material will re-solidify, but will leave defects behind, Jiang

said. "These residual defects will migrate and accumulate to form large scale defects in the long run."

While large defects, such as dislocation loops and voids, can be directly seen using advanced microscopy techniques, many small-scale defects remain invisible even under the best microscopes. These small defects can significantly impact the materials, making the use of computer simulations to fill this knowledge gap critical. INL computational scientists combine their simulations with the advanced characterization techniques performed by material scientists at INL's Materials and Fuels Complex to advance the understanding of material behavior in a nuclear reactor.

### SIMULATING THE IMPACTS OF EARTHQUAKES ON REACTOR MATERIALS

Another INL scientist, Chandu Bolisetti, also simulates damage to materials, but on a much different scale.

Bolisetti, who leads the lab's Facility Risk Group, uses high-performance computing to simulate the effects of seismic waves — the shaking that results from an earthquake — on energy infrastructure such as nuclear power plants or dams.

In early 2021, funded by the DOE Office of Technology Transitions, Bolisetti and his colleagues performed a particularly complex type of simulation — they simulated the impacts of seismic waves on a nuclear power plant building that houses a molten-salt reactor.

A molten-salt reactor is a particularly difficult physics problem because the coolant/fuel circulates through the reactor in liquid form. The team also placed their hypothetical reactor on seismic isolators, giant shock absorbers that help reduce the impacts of earthquakes on buildings.

MASTODON is a MOOSE-based modeling and simulation code used to model how earthquakes can affect nuclear power plants.

Bolisetti's team ran the simulation using MOOSE, which stands for Multiphysics Object Oriented



MASTODON is a MOOSE-based modeling and simulation code used to model how earthquakes can affect nuclear power plants.

Simulation Environment, a software framework that allows researchers to develop modeling and simulation tools for solving multiphysics problems. For these earthquake simulation problems, Bolisetti's team uses MASTODON, which they developed using MOOSE specifically for seismic analysis.

Another project led by Bolisetti and funded by INL's Laboratory Directed Research and Development program looks at how a molten-salt reactor behaves in an earthquake in much more detail. It extends the analysis to include neutronics and thermal hydraulics — in other words, how the shaking impacts nuclear fission and the distribution of heat in the reactor core.

"All three of these physics — earthquake response, thermal hydraulics and neutronics — are pretty complicated," Bolisetti said. "No one has ever combined these into one simulation. How the power in the reactor fluctuates during an earthquake is important for safety protocols. It affects what the operators would do during an earthquake and helps us understand the core physics and design safer reactors."

"Real world experiments to simulate this are close to impossible, especially when you add neutronics," Bolisetti said. "That's where these kinds of multi-physics simulations really shine."



## SIMULATING NUCLEAR ROCKETS FOR A TRIP TO MARS

Mark DeHart, a senior reactor physicist at INL, uses MOOSE to simulate an entirely different kind of complex machine: a thermonuclear rocket that could someday take humans to Mars.

The rocket would use hydrogen as both a propellant and a coolant. When the rocket is in use, hydrogen would run from storage tanks through the reactor core. The reactor would rapidly heat the hydrogen before it exits the rocket nozzles.

"The hydrogen that comes out is pure thrust," DeHart said.

Compared with chemical rockets, thermonuclear rockets are faster and twice as efficient. The rockets could cut travel time to Mars in half. One big challenge is rapidly heating the reactor core from about 26 degrees Celsius to nearly 2,760 Celsius without damaging the reactor or the fuel.

DeHart and his colleagues are using Griffin, a MOOSE-based advancedreactor physics tool, for multiphysics modeling of two aspects of the NASA mission.

The first project simulates the fuel's performance as it experiences rapid heating in the reactor core. The real-world fuel samples are placed in INL's TREAT where they are rapidly brought up to temperature.

The data from those experiments are used to create and validate models of the fuel's neutronics and heat-transfer characteristics using Griffin.

"If we can show that Griffin can model this real world sample correctly, we can have confidence that Griffin can calculate correctly something that doesn't exist yet," DeHart said.

The second project is designing the rocket engines themselves. Automated controllers rotate drums in the reactor core to bring the temperature up and down. "We've developed a simulation that will show how you can use the control drums to bring the reactor from cold to nearly 5,000 F within 30 seconds," DeHart said.

Without high-performance computing and MOOSE, developing a thermonuclear rocket would take dozens of experiments costing hundreds of millions of dollars.



### AN OPPORTUNITY FOR COLLABORATION

In the end, high-performance computing makes INL a gathering place for researchers with a wide range of expertise, from rocket design to artificial intelligence. About half the system's users are from national labs, with a quarter coming from universities and a quarter from industry. The resulting collaborations are especially important for nuclear energy research.

"INL cannot attract all the experts in our field, but by sharing a computer, INL's team can work with 1,200 experts across the United States," Whiting said. "INL's supercomputers are helping build the expertise and develop the tools so they can deploy next-generation reactors."

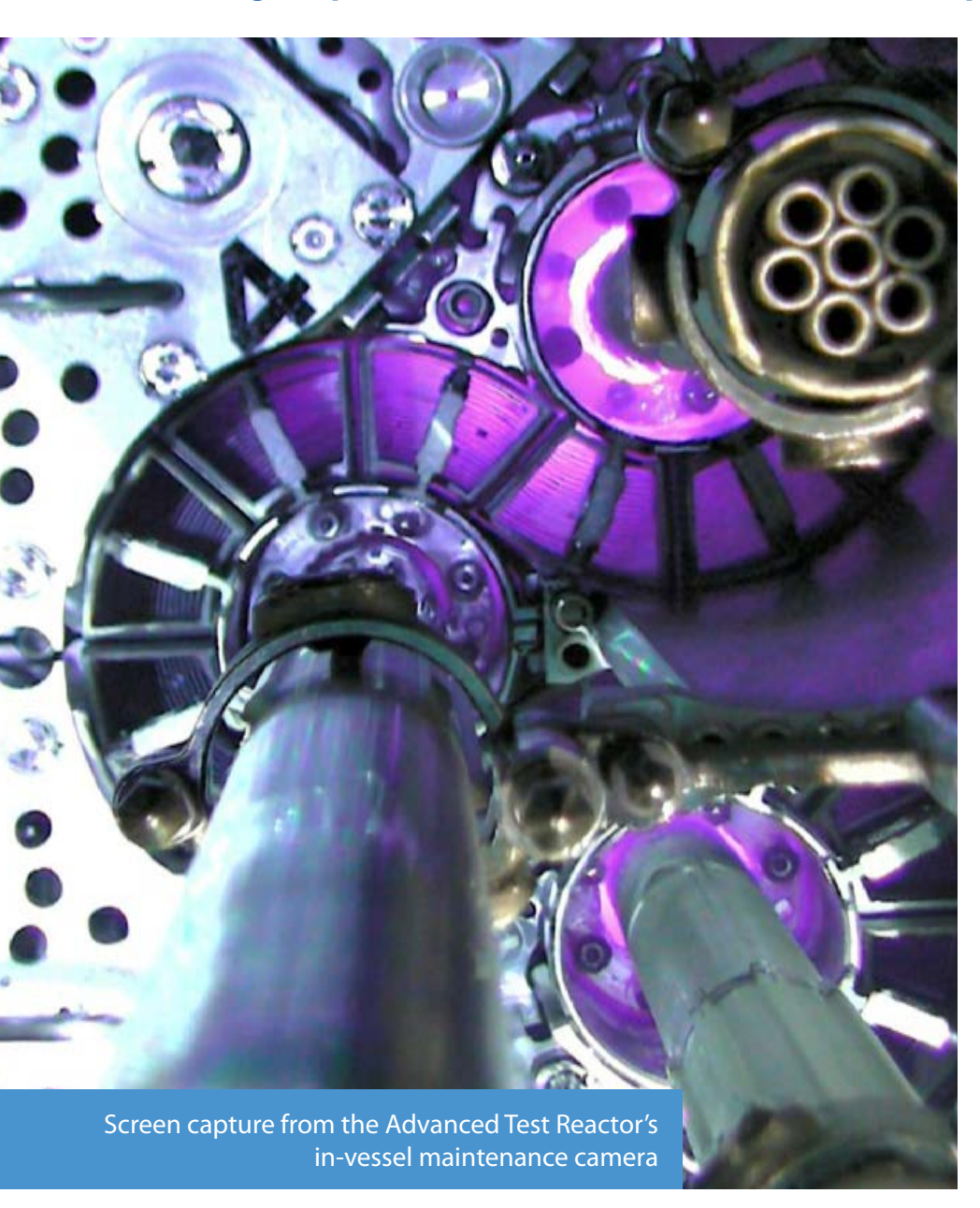
"We need years of research with the High-Performance Computing facility," said Jiang. "We need to understand the high energy state of nuclear materials as accurately as possible, so we need to explore a huge space. Without highperformance computing, basic energy research would suffer. It's critical."

And the demand for these modeling and simulation resources is only growing. Sawtooth added more than four times the capacity to INL's high-performance computing capabilities, and already the line of projects waiting in the queue can reach into the thousands.

If you are interested in accessing INL's supercomputers for your work, visit inl.gov/ncrc or nsuf.inl.gov.

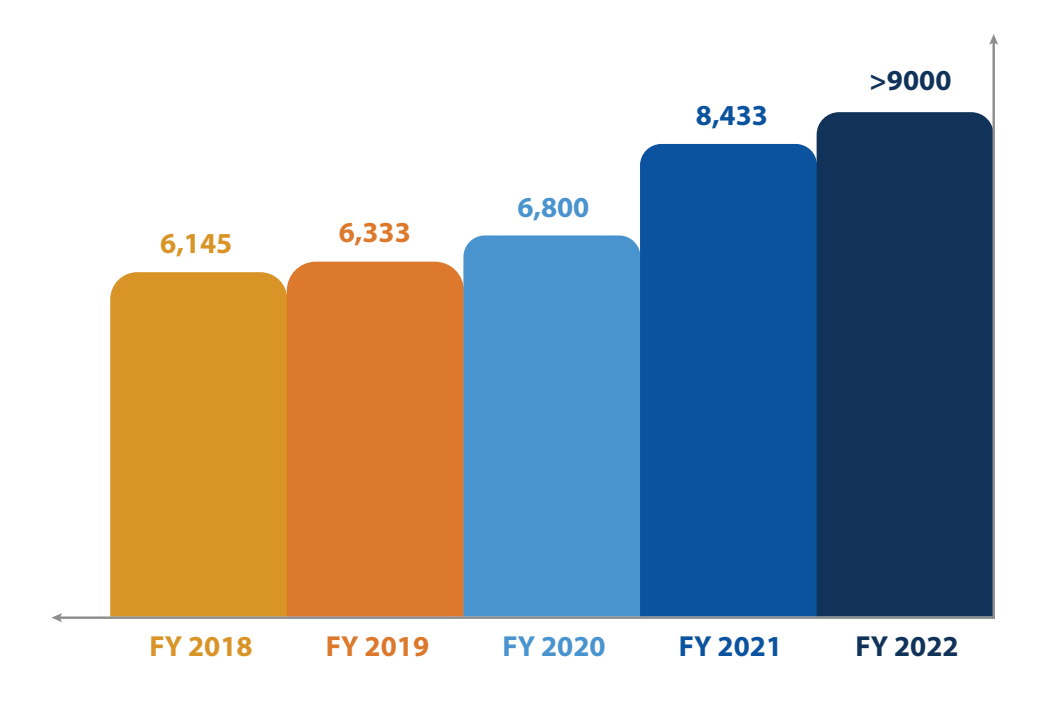
# MATERIALS LIBRARY

#### Curating irreplaceable fuels and materials for nuclear power research.



With the addition of unique, nuclearenergy-relevant samples to its inventory and a more prominent presence within the national and international nuclear community, the Nuclear Fuels and Materials Library (NFML) continues to grow in recognition as the foremost archive of nuclear research samples and material.

The NFML, owned by the U.S. Department of Energy's Office of Nuclear Energy and curated by the NSUF, is the largest global open archive of high-value irradiated fuel and material samples. It includes samples from real-world components retrieved from decommissioned power reactors, archived material from irradiation testing projects, and donations from other sources. As shown in the graphic on the following page the NFML's sample inventory has continued to increase over the years.



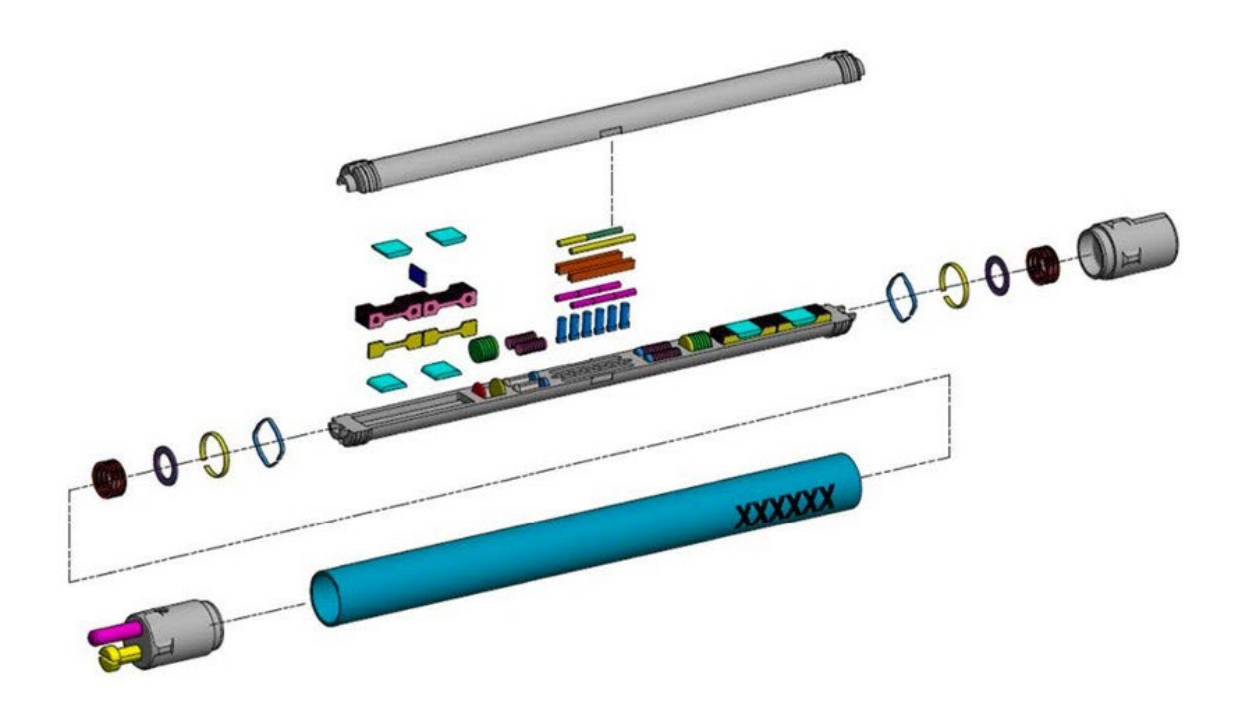
NFML FY 2022 sample inventory growth.

### THE SAMPLE-2 (SAM-2) CAMPAIGN

The NSUF performs periodic irradiation campaigns to populate the NFML with samples for future investigations and fill gaps in the current inventory. For example, SAM-2 is a non-fueled drop-in materials experiment that irradiates high-purity silicon carbide (SiC) specimens. This experiment will provide insight into the complex inter-relationship between the electronic structure and the thermal and mechanical properties of phosphorous-doped, high-purity SiC. The irradiation will continue for multiple cycles in the Advanced Test Reactor, with individual capsules independently removed upon

achieving a predetermined neutron dose. Three of eight capsules have achieved the target doping level and were removed from the Advanced Test Reactor in FY 2022. They will be available in the library in 2025 or when post-irradiation examination is completed.

SAM-2 was the first experiment to utilize the team's specific capsule design. This design is being developed as a standard option for all users that will save substantial time and money in future irradiation experiments by equipping investigators with an approved design for tensile bars and 3- and 6-mm disc samples, which are the most utilized specimen sizes.



#### **SERVING AS A REPOSITORY**

The NFML, increasingly recognized as a repository for a diverse selection of nuclear fuels and materials, is a valuable resource to the nuclear research community. Adding material assets to the NFML safeguards them from being disposed of as waste or lost to long-term storage. As the curator of valuable unused or residual fuels and materials, the NSUF maintains the physical inventory and material provenance, ensuring that the samples and associated information remain available to future researchers. New additions donated to the library by external sources offer new opportunities for future nuclear researchers to continue advancing the nuclear energy mission without performing new test-reactor irradiation campaigns.

The NFML was recognized and sought out as a repository by colleges, national laboratories, and industry since early in the NSUF and continues throughout FY 2022. Many of the newly offered materials and samples are progressing toward official transfer. However, reviewing the relevance of and accepting offered material, gathering provenance information, and finalizing the official transfer of donated materials have proven to be arduous and time-consuming. Two acquisition efforts that began more than three years ago were concluded in FY 2022, resulting in the accomplishment of a Level 2 milestone and the addition of unique, invaluable samples irradiated in a commercial nuclear power plant and an international research reactor.

#### **PICKING UP SPEED**

The original library catalog consisted of several spreadsheets with an inventory of approximately 3,500 samples. It now includes over 9,000 samples cataloged in a searchable online database. As NSUF projects are completed and examined, unused and archive specimens are added to the library. Sample donations to the NFML have increased alongside the overall value to the nuclear community due to providing access to a collection of unique, real-world samples that otherwise might be lost or destroyed.

Irradiations from NSUF-funded projects resulted in the addition of many relevant samples to the NFML in FY 2022, with more to come in the next three to five years as more NSUF irradiation projects are completed.

Government, academia, and industry recognize the NFML as an invaluable resource that will continue to responsibly curate fuels and materials to ensure that nuclear power is a safe, cost-effective, and sustainable energy solution.



# LABORATORY





The new Activated Materials Laboratory at Argonne National Laboratory (credit, Argonne National Laboratory).

### Improving accessibility, productivity, and capabilities: The Activated Materials Laboratory

An upgrade is in progress to generate X-rays up to 500 times brighter than the ones the Advanced Photon Source (APS) produces now, opening the door to scientific discovery on a scale we have yet to imagine. Even before the upgrade, the APS, housed at Argonne National Laboratory, was one of the world's top X-ray light sources.

In progress since June 2020 and completed this summer, the Long Beamline Building (LBB) is home to two stations where researchers will carry out cutting-edge experiments using the brighter X-ray beams. The LBB will host the unique Activated Materials Laboratory (AML), which can safely prepare and dispose of materials used in experiments conducted in a facility. Proud to enable scientific discoveries, the **Nuclear Science User Facilities** (NSUF) provided funding for the design, construction and operation of the AML.

Not only will the AML facilitate the safe handling and storage of radioactive materials, it will provide improved sample accessibility, flexible operation, minimized cycle time, enhanced productivity, and expansion of *in situ* testing capabilities.

As the name implies, the beamlines housed in the LBB are unusually long. A distance of nearly two football fields in length allows for more focused beams and greater detail.

To allow the installation and commissioning of various components, the APS will pause operations for one year, starting in April 2023. Then, when experiments resume in 2024, the beamlines will be immediately available.

U.S. Secretary of Energy Jennifer Granholm attended the ribboncutting ceremony for the LBB in July.



"When America leads on science, we boost our global competitiveness, and we create jobs," said Secretary Granholm, "The newly unveiled facility at Argonne National Lab's Advanced Photon Source is exactly what scientific leadership looks like, and DOE could not be more proud of the scientists, researchers, staff and students who lead this important work."

#### **CAPABILITIES AT A GLANCE**

The Activated Materials Laboratory:

- A radiological facility providing encapsulated radioactive samples for characterization at the Advanced Photon Source beamlines
- Handling nuclear materials and fuels in solid form
- Two fume hoods and two gloveboxes
- · Lead-lined storage cabinet
- Receiving and shipping samples
- (Dis)assembling sample containment
- Testing and maintaining in situ equipment

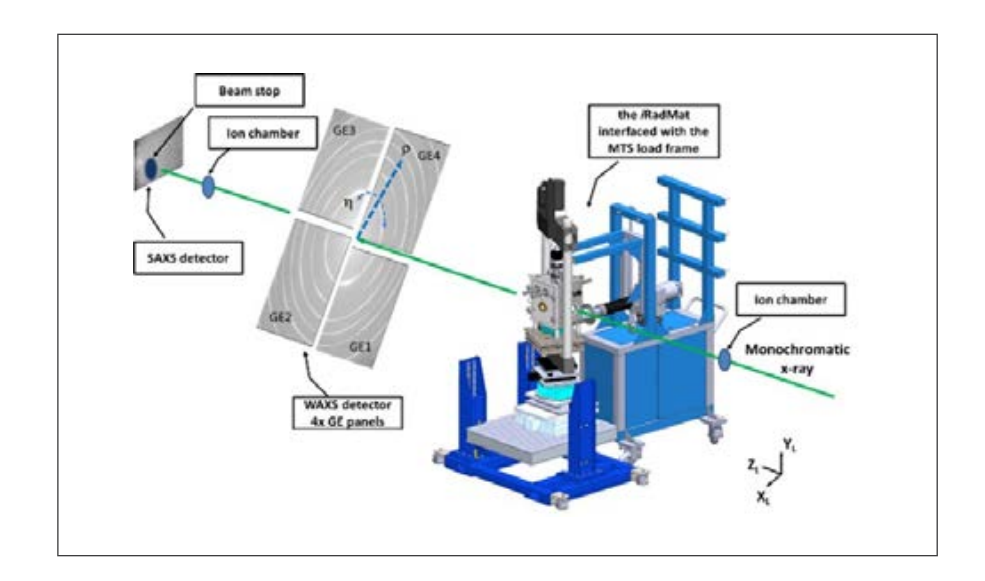
### THE IN SITU RADIATED MATERIALS MODULE<sup>[1]</sup>

- Tungsten and molybdenum lined chamber
- High-temperature (up to 1200°C) vacuum (1×10-5 Torr level) furnace
- X-ray/optical windows on four sides
- Designed as an insert to the MTS Model 858 load frame
- In-grip rotation-tension mechanism

[1] X. Zhang et al. Review of Scientific Instruments, 88 (2017) 015111

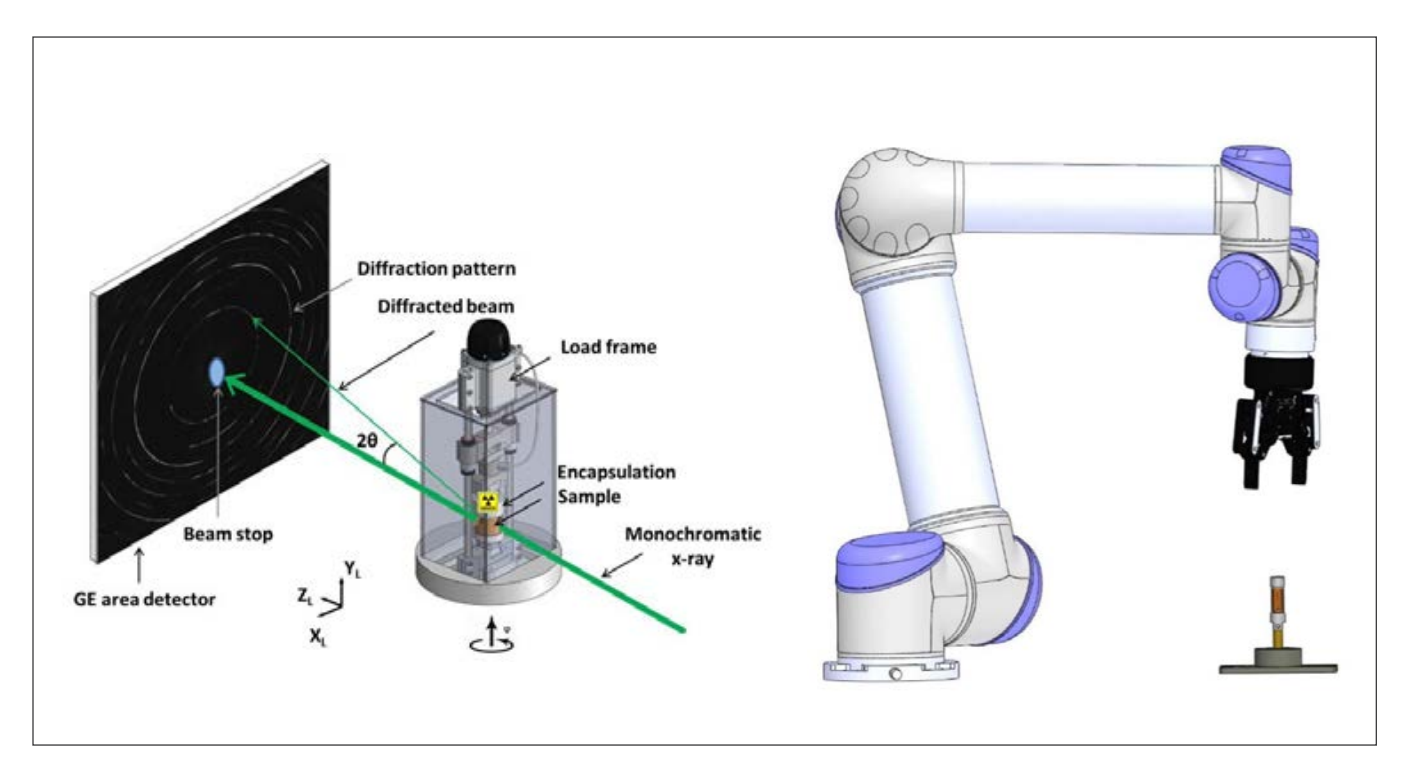
### **SAMPLE ENCAPSULATION**

- Various double encapsulation designs
- Design concepts available for room-temperature tests, hightemperature tests, in situ and ex situ experiments









### THE COMPACT LOAD FRAME

- Psylotech µTS microtest system with customized features
- Compatible with tension, compression and fatigue tests
- Can be placed on translation and rotation stages at the beamline for three-dimensional (3D) measurement
- · Maximum load of 5 kN
- Room-temperature, air tests only
- Customized grips for radioactive samples

### THE ROBOTIC ARM

- Universal Robots UR5 model
- Compact tabletop machine that weighs 11 kg
- Maximum payload of 5 kg
- · Maximum reach of 850 mm
- 360-degree rotation on all wrist joints

# NSUF TEAM



### **ALINA ZACKRONE**

Alina Zackrone is the new postirradiation examination (PIE) experiment manager for the NSUF. Alina manages all PIE scope for Consolidated Innovative Nuclear Research and Rapid Turnaround Experiment projects.

When asked to what personality traits she most attributes her success, Alina said, "The personality trait that has helped me succeed is a stubbornness to understand people and problems. This has driven me to continuously learn how to solve problems better and relate to people. "This trait has maintained a valuable position in her career: "In project management and previous positions, it has been a beneficial trait, as new problems are continually emerging that require creative solutions."

Alina's mother gave great advice that has followed her throughout her professional career. "Give everything at least three good tries," said Alina. She mentioned that this has been helpful both with hobbies and in her professional life.

"Very rarely do you understand something after seeing it once.
Normally, if you fail once, the lessons you learn will only increase your chances of success the next time."

Alina enjoys playing with her dog when away from work and snowboarding on fresh powder, open to close. "There is nothing quite like the feeling of being in nature, floating through snow and spending quality time with people at a ski resort," said Alina.





### **MATTHEW ANDERSON**

Matthew Anderson is the manager for High-Performance Computing (HPC) at Idaho National Laboratory. He maintains the highest operational performance and security level for all the HPC systems while lowering the threshold for usage to non-experts through training and software development.

Matt is proud of the deployment of the Open OnDemand science gateway. OnDemand allows users to access HPC files, open shells, access Linux desktops, use other interactive apps, and build job submissions to submit to a cluster from a web browser. Users given permission by the OnDemand web portal can use Level One code access.

A great piece of advice he's received is that "90% of high-performance computing is just plumbing."

We asked if he has any hidden talents or hobbies and were surprised to find out that Matt fixes and services pianos on weekends.

### **MEGAN BROADHEAD**

Megan Broadhead is NSUF's new planning and financial-controls specialist, providing overall planning and financial controls support to NSUF. She monitors the budget, costs, and ensures approved funding is maintained.

The best advice she ever received was from a former boss while discussing goals and career aspirations. He told her, "You'll never get started if you never get started." Even though it may seem like common sense, it's a good reminder to keep taking steps toward the things you want, and it's a piece of advice that Megan always goes back to.

This year, Megan would like to visit some of the incredible natural wonders Idaho has to offer.





### **RONGJIE SONG**

Rongjie Song is a metallurgical engineer at Idaho National Laboratory. This means she works towards developing a mechanistic understanding of composition, manufacturing, microstructure, and property relationships in nuclear structural materials. Her role emphasizes microstructure evolution and mechanical properties in harsh environments such as irradiation, high-temperature, mechanical stress, and corrosive environments.

While away from work, Ronjie enjoys long walks, playing games, and spending time with family.

### **AARON RUSSELL**

Aaron Russell creates and executes irradiation experiment schedules, scopes, and budgets from project initiation through final project closeout as an experiment manager.

When asked what behavior or personality trait he most attributes his success to, he told us that he is interested in understanding the larger picture. He moved into project management after working as an engineer for a few years. He can see how all the interrelated moving parts interact and affect each other, whether that be the company's inner workings or the many aspects of a project. This has helped him successfully focus on the critical path that need the most attention to ensure a project's success.

In general, Aaron enjoys playing sports and working out. "Tennis and pickleball are my current obsessions. I enjoy fantasy football and strategic board games. Also, I recently got into chess," said Aaron.





### **ERIC WHITING**

Eric Whiting is the division director for Advanced Scientific Computing at INL. He plays a role in enabling the INL mission by providing scientific computing resources such as supercomputers, software to support modeling and simulation, and expertise and tools in artificial intelligence, data, and visualization. He has a remarkable ability to listen, think about the big picture, and come up with solutions to technical problems.

Aiding in the design and construction of the Collaborative Computing Center has been a massive accomplishment for Eric and the NSUF team. When asked about misconceptions surrounding his work, Eric said, "people think buying and installing a supercomputer is an easy process."

He enjoys getting outside, mountain biking up obstacles such as stairs, inventing, and fixing things.

# PROJECTS

### **Awarded Consolidated Innovative Nuclear Research projects**

Project Title	Principal Investigator	PI Organization	NSUF Facilities
Mechanical response and chemical effects at the fuel-cladding interface of HT-9 and metallic fuel	Maria Okuniewski	Purdue University	Hot Fuel Examination Facility and Irradiated Materials Characterization Laboratory at Idaho National Laboratory; High-Performance Computing at Idaho National Laboratory
Accelerated irradiation and evaluation of ultrastrong and elastic glassy carbon	Junhua Jiang	Idaho National Laboratory	Analytical Chemistry Laboratory and Microscopy and Characterization Suite at Center for Advanced Energy Studies; Irradiated Materials Characterization Laboratory at Idaho National Laboratory; Accelerator Laboratory at Texas A&M University
Gamma irradiation effects on the mechanical behavior of seismic protective devices	Andrew Whittaker	Univeristy of Buffalo	Electron Microscopy Laboratory and Irradiated Materials Characterization Laboratory at Idaho National Laboratory
Accelerated irradiation and evaluation of ultrastrong and elastic glassy carbon	Gabriel Meric	Kairos Power, LLC	Irradiated Materials Characterization Laboratory at Idaho National Laboratory; Massachusetts Institute of Technology Nuclear Reactor Laboratory at Massachusetts Institute of Technology



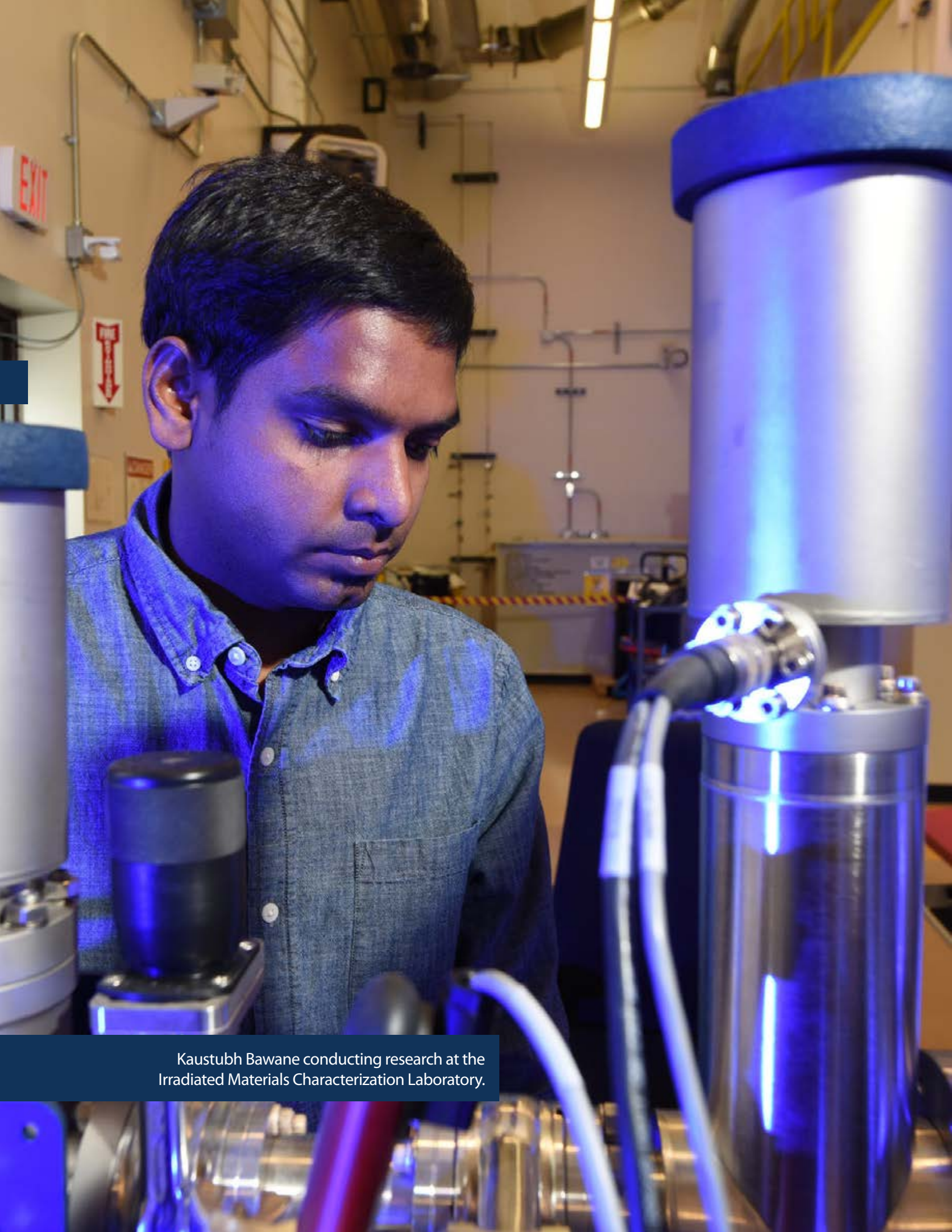
### **Awarded Rapid Turnaround Experiments**

Project Title	Principal Investigator	PI Organization	NSUF Facilities
Effects of the fabrication technique and composition on microstructural evolution in uranium-molybdenum alloys neutron irradiated up to 1 dpa at low temperatures.	Maria Okuniewski	Purdue University	Post-Irradiation Examination using National Synchrotron Light Source II at Brookhaven National Laboratory; Sample Preparation andhipping using Electron Microscopy Laboratory at Idaho National Laboratory
Characterization of irradiation effects on the electrical resistance of tungsten	Dan Floyd	University of Tennessee- Knoxville	Sample irradiation using Ohio State University Research Reactor at The Ohio State University
Microstructural characterization of the SiC-SiO <sub>2</sub> interface of oxidized TRISO particles	Katherine Montoya	University of Texas-San Antonio	Post-Irradiation Examination using Low Activation Materials Design and Analysis Laboratory at Oak Ridge National Laboratory
Dislocation loop and bubble evolution in helium irradiated ${\rm ThO_2}$ and ${\rm UO_2}$ single crystals	Marat Khafizov	The Ohio State University	Post-Irradiation Examination using Microscopy and Characterization Suite at Center for Advanced Energy Studies; sample irradiation using Accelerator Laboratory at Texas A&M University
Grain boundary evolution during irradiation in RPV steels	Emmanuelle Marquis	University of Michigan	Post-Irradiation Examination using Microscopy and Characterization Suite at Center for Advanced Energy Studies
Neutron irradiation effects on the tensile properties of wire arc additive manufactured Grade 91 steel	Theresa Green	University of Michigan	Irradiated Materials Examination and Testing Facility at Oak Ridge National Laboratory
Radiation tolerance of advanced multilayered coatings under transient temperature conditions	Yinbin Miao	Argonne National Laboratory	Intermediate Voltage Electron Microscopy Tandem Facility at Argonne National Laboratory
Atom probe and transmission electron microscopy studies on neutron irradiated FeCrMnNi compositionally complex alloy	Adrien Couet	University of Wisconsin	Irradiated Materials Characterization Laboratory at Idaho National Laboratory

Project Title	Principal Investigator	PI Organization	NSUF Facilities
Investigation of spinel phase formation on Ni-doped FeCrAl alloy in radioactive hydrogenated water	Yi Xie	Purdue University	Michigan Center for Materials Characterization at University of Michigan
Examining microstructures and mechanical properties of neutron and ion irradiated T91, HT9 and 800H alloys	Pengcheng Zhu	University of Tennessee- Knoxville	Low Activation Materials Design and Analysis Laboratory at Oak Ridge National Laboratory
Irradiation effects on unexpected deformation-induced martensitic phase transformation in Ni-alloys	Caleb Clement	Purdue University	Microscopy and Characterization Suite at Center for Advanced Energy Studies; Michigan Ion Beam Laboratory at University of Michigan
In situ TEM ion implantation characterization on helium bubble formation in iron-phosphate nuclear waste glass immobilizing salt waste streams	Ming Tang	Clemson University	Intermediate Voltage Electron Microscopy Tandem Facility at Argonne National Laboratory
Electron probe microanalysis of localized phases in irradiated U-10 wt%Zr alloy fuel	Luca Capriotti	Idaho National Laboratory	Irradiated Materials Characterization Laboratory at Idaho National Laboratory
lon irradiation and characterization of FeCrAl oxide dispersion strengthened alloy manufactured via laser powder bed fusion	Somayeh Pasebani	Oregon State University	Microscopy and Characterization Suite at Center for Advanced Energy Studies; Accelerator Laboratory at Texas A&M University
An assessment of radial compositional variations of the grey phase in FBR MOX fuel using EPMA	Casey McKinney	University of Florida	Irradiated Materials Characterization Laboratory at Idaho National Laboratory
Fission product partitioning behavior in irradiated monolithic U-Mo fuels	Charlyne Smith	Idaho National Laboratory	Irradiated Materials Characterization Laboratory at Idaho National Laboratory
Atom probe characterization of oxide and metal/oxide interface on proton irradiated Zry-4 after exposure in high-temperature water	Peng Wang	University of Michigan	Microscopy and Characterization Suite at Center for Advanced Energy Studies

Project Title	Principal Investigator	PI Organization	NSUF Facilities
Radiation-induced attenuation and nonlinear optical properties of fused silica and single-crystal sapphire	Milos Burger	University of Michigan	Irradiated Materials Examination and Testing Facility at Oak Ridge National Laboratory
Irradiation behavior of nanostructured ferritic/martensitic Grade 91 steel at high dose	Haiming Wen	Missouri University of Science and Technology	Microscopy and Characterization Suite at Center for Advanced Energy Studies; Michigan Ion Beam Laboratory at University of Michigan
Radiation tolerant neuromorphic computing system using 3-D NAND flash memory	Biswajit Ray	University of Alabama	Advanced Test Reactor at Idaho National Laboratory; The Ohio State University
In situ TEM studies on thermodynamic stability and microstructural evolution of zirconium hydrides in irradiation and thermal environments	Caitlin Taylor	Los Alamos National Laboratory	Intermediate Voltage Electron Microscopy Tandem Facility at Argonne National Laboratory
Hydrogen-retention of yttrium hydride under high-temperature proton irradiation	Timothy Lach	Oak Ridge National Laboratory	Low Activation Materials Design and Analysis Laboratory at Oak Ridge National Laboratory; Michigan Ion Beam Laboratory at University of Michigan
Atom probe tomography and transmission electron microscopy studies on LWR-irradiated harvested reactor internals	Patrick Purtscher	Nuclear Regulatory Commission	Irradiated Materials Characterization Laboratory at Idaho National Laboratory
Effect of neutron irradiation on the microstructure of NF616 (Grade 92) as a function of dose and temperature	Indrajit Charit	University of Idaho	Materials Science and Technology Laboratory at Pacific Northwest National Laboratory
Synchrotron characterization of corrosion growth on gamma irradiated aluminum nuclear spent fuel alloys	Trishelle Copeland-Johnson	Idaho National Laboratory	National Synchrotron Light Source II at Brookhaven National Laboratory
<i>In situ</i> irradiation of fission nanoprecipitates	Lingfeng He	Idaho National Laboratory	Intermediate Voltage Electron Microscopy Tandem Facility at Argonne National Laboratory; Irradiated Materials Characterization Laboratory at Idaho National Laboratory

Project Title	Principal Investigator	PI Organization	NSUF Facilities
Irradiation effects on microstructure and mechanical properties in a laser welded ODS alloy	Matthew Swenson	University of Idaho	Microscopy and Characterization Suite at Center for Advanced Energy Studies
Phase reversion analyses in irradiated U-10Zr fuel via <i>in situ</i> experiments	Fidelma Di Lemma	Idaho National Laboratory	Irradiated Materials Characterization Laboratory at Idaho National Laboratory
Micromechanical testing of LWR irradiated harvested reactor internals	Matthew Hiser	Nuclear Regulatory Commission	Irradiated Materials Characterization Laboratory at Idaho National Laboratory
Probing the effect of specific chemical elements on the irradiation induced defects formation and evolution in high entropy alloys	Djamel Kaoumi	North Carolina State University	Intermediate Voltage Electron Microscopy Tandem Facility at Argonne National Laboratory



# REPORTS

hrough its Rapid Turnaround Experiment and Consolidated Innovative Nuclear Research calls, the NSUF grants access to its facilities for researchers to conduct their studies to further the understanding of the effects of irradiation on nuclear fuels and materials.

### **Technical Reports**

Performance of SiC-SiC Cladding and End Plug Joints under Neutron Irradiation with a Thermal Gradient

Understanding Swelling Related Embrittlement of AISI 316 Stainless Steel Irradiated in EBR-II

### **Short Communications**

Ion Irradiation for High Fidelity Simulation of High Dose Neutron Irradiation

IVEM Investigation of Defect Evolution in FCC Compositionally Complex Alloys under Dual-Beam Heavy-Ion Irradiation

ChemiSTEM Characterization of Bulk Heavy Ion Irradiated Complex Concentrated Alloys

Understand the Fission Products Behavior in UCO Fuel Kernels of Safety Tested AGR2 TRISO Fuel Particles by Using Titan Themis 200 with ChemiSTEM Capability

Alumina-stabilized Coatings under Irradiations: Towards Future Generation Nuclear Systems

Evolution of Ga<sub>2</sub>O<sub>3</sub> Native Point Defects, Donors, and Acceptors with Neutron Irradiation

Heavy Ion Irradiation and Characterization of Light-Refractory, Body-Centered Cubic, High-Entropy Alloys

### TECHNICAL REPORTS

## Performance of SiC-SiC Cladding and End Plug Joints under Neutron Irradiation with a Thermal Gradient

Christian Deck - General Atomics - christian.deck@ga.com



his project focused on the fabrication and out-of-pile and in-pile characterization of joining methodologies for SiCbased components. Researchers identified three promising joint formulations to be used to fabricate joint specimens and measure mechanical, thermal, microstructural, high-temperature, and leak performance in both out-of-pile testing and after irradiation. These formulations were transient eutectic phase (TEP), calcia-alumina oxide (CA), and hybrid silicon-carbide (HSiC) preceramic polymer/chemical vapor deposition (CVD) (HSiC). Joint processing methods were developed for a representative cladding tube-end-plug geometry. Tube-end-plug and torsion-joint specimens were irradiated in High Flux Isotope Reactor (HFIR) to ~2 dpa at representative application temperatures (350°C and 750°C).

The HSiC joint formulation showed the best overall performance, considering relevant geometry, irradiation, and temperature effects. Geometry-dependent processing challenges were encountered for both TEP and CA joints. TEP joints were strongest in planar configurations but could not be leaktight in tube-end-plug geometries. CA joints showed lower thermal conductivity than HSiC and TEP joints and experienced a statistically significant loss of strength following irradiation. HSiC and TEP joints retained strength following irradiation.

This project verified first-of-a-kind leak-tight joints following irradiation for CA and HSiC tube-end-plug joints and demonstrated the first use of torsion-joint specimens to obtain thermal data and joint shear strength, increasing the potential data obtained from valuable irradiation specimens.

#### Introduction

The exceptional material properties and irradiation performance of SiC have increased interest in SiC and fiber reinforced (SiC-SiC) composites materials for a range of nuclear applications, including cladding, channel boxes, and structural components in both existing light-water and advanced reactors. However, to demonstrate the use of this material in actual applications,

representative (in size and geometry) components of interest are not feasible to make as a single part; thus., a high-performance, irradiation-tolerant joining process is required. While there has been considerable progress in SiC joining technologies, these initial studies have focused on the irradiation performance of planar joints with respect to strength. Although these have been extremely valuable in screening joint methodologies and understanding joint material degradation in representative irradiation environments, they have not addressed key issues for cladding joints, such as leak tightness and fabrication compatibility in tubular cladding geometries.

The aim of this Nuclear Science
User Facilities funded project,
"Performance of SiC-SiC Cladding
and End Plug Joint under Neutron
Irradiation with a Thermal Gradient"
(Project ID: 17-12573, DOE award:
DE-NE0008720), was to obtain
critical performance data for
SiC joints under irradiation in
representative thermal conditions
and representative joint geometries.

This project demonstrated high-performance SiC joints in relevant geometries that showed exceptional behavior in out-of-pile testing and after irradiation, which supports the deployment of SiC components in nuclear applications.

In addition, the work provided material-property data to enable more-accurate modeling of joints in SiC-based components for nuclear applications. Three different joint types were selected for evaluation based on previous studies of their mechanical stability after exposure to neutron irradiation in planar geometries: TEP, CA and a hybrid (preceramic polymer and CVD) SiC joint (HSiC). In this project, a more comprehensive assessment was conducted of these three promising SiC joints. To evaluate performance, researchers subjected planar and representative cladding tube-end-plug joints to mechanical, thermal, and gas-tightness testing before and after irradiation in HFIR at Oak Ridge National laboratory (ORNL). In addition, researchers performed modeling to simulate joint performance in representative geometries.

### **Project Hypothesis**

Silicon carbide (SiC) composites offer exceptional promise for accident-tolerant fuel cladding applications in current and advanced reactors. Irradiation-tolerant joining methods are necessary to realize SiC-based components; however, demonstrations of irradiation performance on a representative cladding-component geometry still need to be done. This project demonstrated the fabrication of application-relevant joint geometries for three promising joint formulations; characterized the mechanical, thermal, hightemperature, and hermetic out-ofpile performance; updated joint mechanical models; irradiated joint specimens under representative temperatures; and performed post-irradiation examination (PIE) to identify the most-promising joint formulation for nuclear cladding applications.

## **Experimental or Technical Approach**

Three joint formulations were studied and modeled in this work. Researchers selected all three based on prior literature reports, which indicated the joint formulations show potential for stability under certain irradiation conditions and in certain specimen geometries.

The three joint formulations studied were as follows:

### **Transient Eutectic Phase**

This joint formulation uses a mix of SiC powder with smaller quantities of alumina and yttria powders (~10%) to create a material that can melt, flow, and then solidify during processing to form a joint. The team selected lower joining pressure for this study due to compatibility with the specimen geometries of interest. In addition, selecting a specific joint end plug angle that would reduce tube damage during processing in the tube-end-plug specimens was necessary.

### Calcia-Alumina Glass Oxide

Researchers prepared the CA glass-ceramic joint by mixing 50 wt% calcium oxide (CaO) with 50% alumina ( $Al_2O_3$ ) to produce an oxide slurry for application to the joint area. The assembled SiC parts were heated in an inert environment to form the joint.

### **Hybrid Silicon Carbide**

HSiC joints were made by applying a preceramic polymer slurry between the joining surfaces, processing the polymer through a ceramatization heat treatment and then densifying the joint using chemical vapor infiltration (CVI) and CVD.

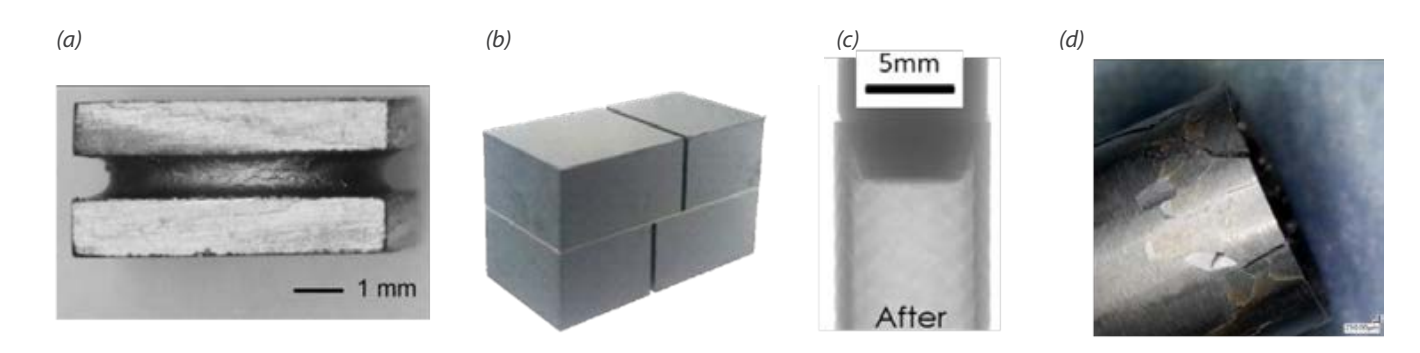


Figure 1: (a) Torsion, (b) DNS, (c) tube-end-plug joint specimens made during project, (d) cracking caused by pressure application during TEP joint processing in tube-end-plug joint scarf geometry showing geometry-dependent fabrication challenges.

Researchers fabricated joint specimens in three configurations. First, the team used torsion hourglass joint specimens for torsion strength testing, thermal diffusivity measurement, and irradiation. The team used double-notch shear (DNS) specimens for high-temperature mechanical testing. Representative tube-end-plug joint samples were developed and used for strength testing, leak testing, nondestructive examination, irradiation exposure, and subsequent PIE. Fabrication of representative tube-end-plug joints was particularly challenging for the TEP joint formulation. The TEP geometry uses a scarf (angled) joint geometry. TEP processing requires pressure application during a high-temperature process step. While processed TEP is very effective for flat planar geometries (such as the DNS specimens), pressure application against the angled joint caused a hoop-tensile stress in the cladding tube due to load transfer, which resulted in damage. The

researchers selected a 20° angle to best accommodate the jointprocessing conditions for CA, TEP, and HSiC.

Researchers then characterized joint performance and measured room temperature mechanicalperformance using torsion shear testing (performed by ORNL) and end-plug push-out testing according to ASTM standard C1862-17. Elevated-temperature joint mechanical testing was performed on DNS specimens, according to ASTM Standard C1469, at room temperature, 300°C, and 750°C. Joint thermal diffusivity was measured on torsion-shear samples using laser flash analysis (LFA) according to ASTM E1461. Upon noticing an overall diffusivity for the torsion sandwich sample, the research team calculated the contribution of the joint material (compared to the monolithic SiC substrates). Thermal conductivity was determined using literature values for density and specific heat. Leak testing

was performed on tube-end-plug joints using a helium-leak detector. Researchers then examined the joint microstructure using X-ray computed tomography (XCT).

Neutron irradiation of torsion and tube-end-plug joint specimens occurred at HFIR at ORNL, and PIE took place in the Low Activation Materials Development and Analysis (LAMDA) facility. ORNL developed four irradiation capsule designs: two for target specimen geometries and two for target irradiation temperatures. The irradiation experiment utilized rabbit capsules inserted into the HFIR flux trap position. The designs were for dry irradiation (with the capsule filled with inert gas), accommodating one tube-end-plug specimen or sixteen torsion specimens per capsule.

The target irradiation temperatures were either 350°C (representative of a light-water reactor [LWR] application) or 750°C (representative of an advanced-reactor application).

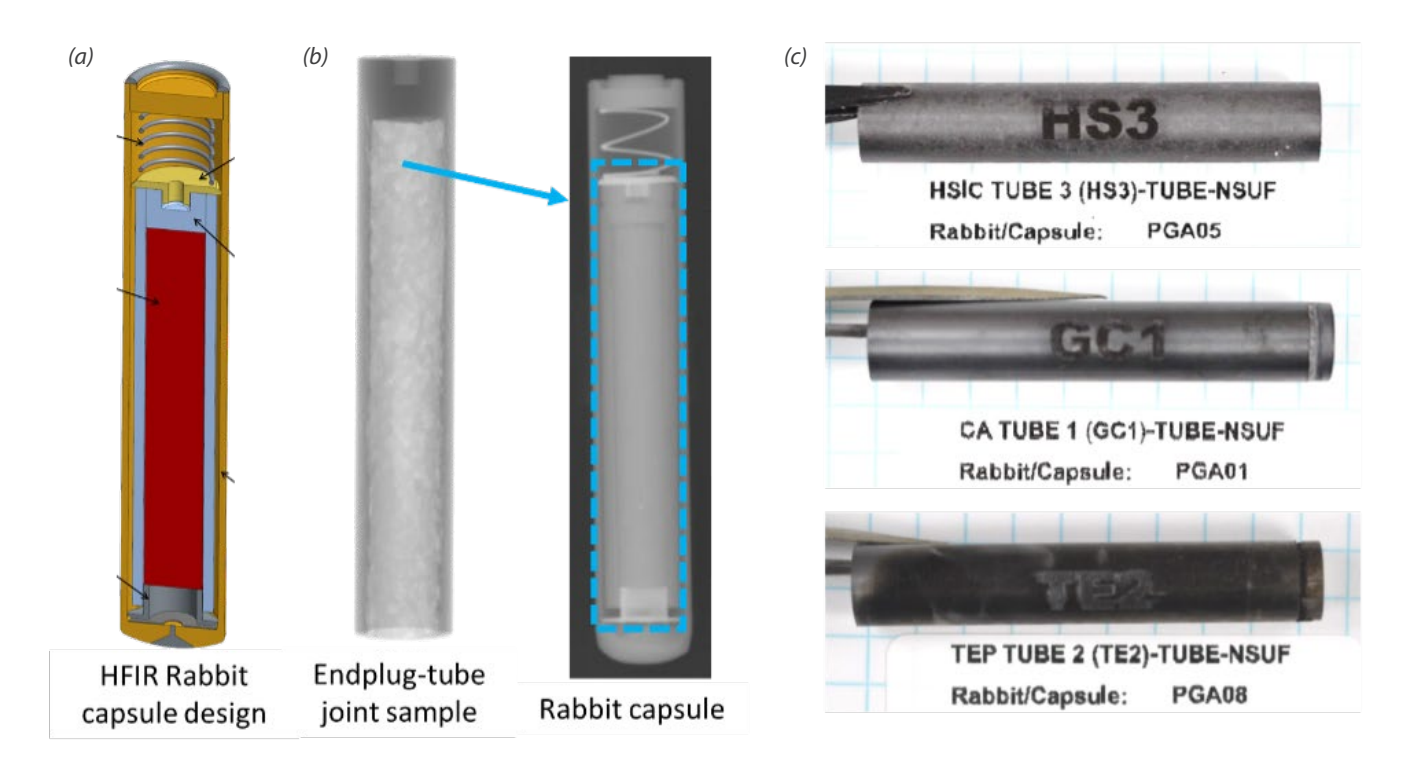


Figure 2: (a) 3D model of the HFIR rabbit capsule design, (b), X-ray images of tube-end-plug specimen and assembled HFIR rabbit capsule, and (c), photographs of irradiated HSiC, CA, and TEP tube-end-plug samples after retrieval from capsules. Joint processing in tube-end-plug joint scarf geometry showing geometry-dependent fabrication challenges.

Three-dimensional thermal analyses were performed using the Ansys finite-element software package to predict temperatures in the specimens during irradiation and temperature distributions inside the joint end plug capsules. These analyses use material-dependent heat-generation rates (heat per unit mass) determined in previous neutronics analyses. The model was used to select a capsule fill gas with 100% He and a 46% He/.Ar balance for the 350° and the 750°C design, respectively.

The team assembled 13 capsules (i.e., two for torsion specimens and 11 for tube-end-plug specimens), accommodating a mix of the TEP, CA, and HSiC joint formulations. All the capsules were inserted in Axial Position 7 of a target-rod rabbit holder in the flux trap of HFIR, targeting an approximate dose of 2 dpa. The team selected this target irradiation dose to reach the saturation condition for SiC and SiC-SiC composites (i.e., temperature dependent, but typically ~1 dpa). The tube-end-plug specimens were irradiated in Cycle 485, and

the torsion-joint specimens were irradiated in Cycle 486. Using dilatometry, researchers investigated the irradiation temperature by post-irradiation annealing of passive SiC temperature monitors. The temperature monitors were irradiated in contact with the substrates of the joint specimens. Following irradiation, disassembly of the 13 capsules occurred in Hot Cell #6 of the Irradiated Materials **Examination and Testing Facility** (IMET) at ORNL. The team then sent all specimens and thermometry to the LAMDA for PIE and analysis.

### **Results**

Results, measurements and observations from this project are summarized in the following:

End-plug push-out (EPPO) testing determined joint strength in tube geometries, with average nominal burst pressures of 26 MPa for HSiC, 36 MPa for TEP, and 58 MPa for CA joint specimens. All joint formulations showed strength values sufficient to survive expected end-of-life internal pressures, and all the formulations met the minimum target strength. The strength of the TEP joint was lower than expected based on the literature. These findings suggest that the method for TEP joining in cladding geometry may have compatibility issues in a representative tube-end-plug geometry and is consistent with the challenges observed in applying pressure to an angled end plug without damaging the tube during join processing. Pressure at the joint interface may not be uniform, leading to local weak spots. The varied pressure can be due to slight geometric misalignment, nonuniform distribution of joint material, or roughness in the composite joining surface.

The DNS specimens showed lower room-temperature shear strengths compared to the torsion testing of the same nominal joint formulations found in the literature. Depending on the test method, it is typical to see varying shear strength. In the case of DNS testing, stress concentrators in the joint region can

affect measured strengths. While the overall shear strengths were lower, the trends in the data compared well with the literature. The HSiC and CA joints showed similar shear strengths, and the TEP joint performed noticeably better. The TEP samples demonstrated excellent mechanical stability up to 300°C, and while the samples retained strength, they did show a drop in performance at 750°C. The HSiC DNS testing showed a very stable mechanical response as a function of testing temperature. The joint is entirely SiC, and the literature shows similar results for tube-end-plug ioints.

Torsion-shear testing showed the highest strengths for TEP joints (169 MPa) and similar for HSiC and CA joints (71 and 80 MPa, respectively). Overall, these mechanical results show that all three selected joint methodologies result in cladding joints capable of withstanding the expected joint mechanical stresses in an LWR environment.

Researchers completed helium leak testing of the joint regions on tube-end-plug specimens to assess the suitability of each joint methodology for cladding applications, which require gas tightness. Only the HSiC approach showed consistent passing leak rate cladding joints. Only HSiC joints consistently passed leak testing. On the other end of the spectrum, the TEP approach was ineffective in producing gas-tight joints. Every tested TEP joined tube failed a bubble test. The test failure

is likely related to combining the required pressure while joining and the representative tube-end-plug geometry (rather than a planar joint specimen). It was difficult to load a thin-walled tube to the required pressures needed to form a TEP joint, and the higher the load, the more risk of damaging the tube. These results suggest that additional technological development is required for TEP joining to be suitable for cladding geometry. The CA joint approach had more mixed results. It performed much better than the TEP samples, with all 10 samples passing the bubble test. However, subject to the helium leak-rate test, only four samples passed below the allotted leak rate requirement. Fabrication variability may contribute to inconsistent joint performance regarding gas tightness.

The research team measured thermal diffusivity for all three joint formulations using torsion hourglass specimens. Researchers used this data to calculate thermal conductivity versus temperature. Next, they measured the thermal conductivity for the CA joint formulation to be guite low. The thermal conductivities of the CA joint constituents (calcium oxide and alumina) are lower than those of the main constituent of the HSiC and TEP joints (SiC). In addition, the team observed the CA joints contained a higher occurrence of internal porosity. The thermal conductivity of the as-fabricated TEP and HSiC joints was considerably larger than that of the CA joints.

Forty-three joint specimens were fabricated and then irradiated in the HFIR at ORNL. Pre-irradiation characterization established a baseline for comparison after irradiation. The irradiation was conducted to ~2 dpa of irradiation damage at either representative LWR (target of 350°C) or representative advanced-reactor temperatures (target of 750°C). One TEP tube-end-plug joint failed during capsule assembly, and another TEP tube-end-plug joint failed either during irradiation or disassembly.

The irradiation temperatures were experimentally determined using SiC thermometry samples. For the tube-end-plug joint specimens, the temperature monitor inside the tube measured temperatures that ranged from 430-450°C for the lower-temperature capsules and between 690-930°C for the highertemperature capsules. Researchers estimated the irradiation temperature for the torsion joint specimens (with sixteen joints per capsule) based on the minimum and maximum irradiation temperatures of multiple SiC temperature monitors in the same irradiation vehicle.

The low-temperature rabbit showed uniform irradiation temperature (250–270°C). Unexpectedly, the high-temperature rabbit exhibited a non-uniform irradiation temperature (530–720°C). These temperatures were slightly lower than the target.

As part of PIE, researchers performed an LFA on a subset of the torsion joint specimens. Before the destructive testing of torsion specimens, the team measured thermal diffusivity across the specimens' full thickness, including both the substrate and joint material. They made thermal-diffusivity measurements for seventeen torsion specimens, covering all three joint formulations (i.e., six CA, six TEP, and five HSiC) and irradiation temperatures (ten specimens between 250–270°C and seven specimens between 530–720°C). The data obtained represented the overall thermal diffusivity through the thickness of the complete assembled specimen (through the joint and both CVD SiC substrate pieces). Researchers analyzed the PIE diffusivity results to calculate the contribution to the diffusivity of the joint and interface based on the assumed diffusivity changes to the CVD SiC substrates. They calculated the joint's thermal conductivity and interface as a function of the joint diffusivity, density, and specific heat.

As expected, the thermal conductivity in the joint generally decreases with exposure to irradiation due to the formation of irradiation-induced defects in the material that impedes heat transfer. TEP has the highest starting conductivity of ~10–25 W/m-K (temperature dependent) due to its composition of ~90% pure high-density SiC. The HSiC material is a 100% pure SiC material but contains residual porosity; therefore, starting

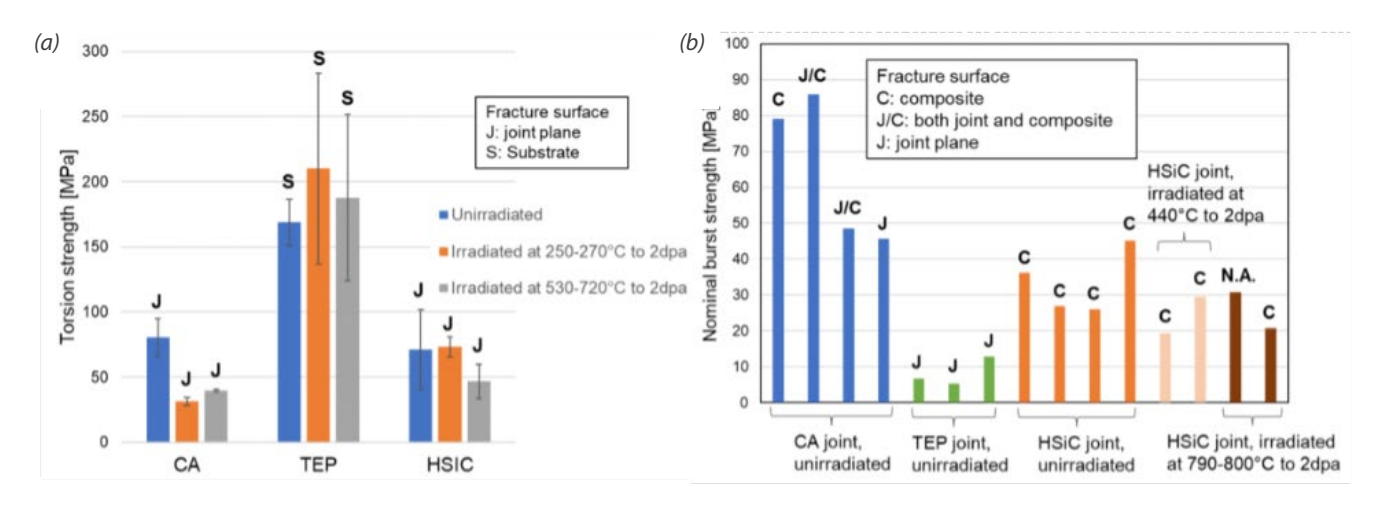


Figure 3: (a) Torsion strength of unirradiated and irradiated SiC joints, (b) EPPO strength of unirradiated tube-end-plug joints and irradiated HSiC tube-end-plug joints.

conductivity values are lower than TEP while still relatively high at ~10 W/m-K. The oxide material has the lowest starting conductivity, only 1-2 W/m-K. After irradiation, reduced conductivity differences between the joint formulations can be observed. The TEP and HSiC joint formulations remain higher than the CA joint material, but the TEP and HSiC conductivities dropped to  $\sim$ 3–6 W/m-K. The degradation of the TEP and HSiC joint material is more pronounced at the lower irradiation temperatures as swelling and defect accumulation (and a corresponding reduction in thermal conductivity) are higher when SiC is irradiated at lower temperatures. The CA joint material conductivity was unchanged; it was low before and after irradiation. The fixed conductivity is attributed to the relative insensitivity of an amorphous glass phase to the accumulation of defects impeding

heat transfer (the irradiation damage effect on an amorphous structure is not as significant as it is on a crystalline structure).

Following LFA of the torsion joint specimens, researchers performed destructive mechanical torsion shear testing to measure the joint shear strength. This testing was a first-of-a-kind demonstration using torsion specimens for thermal and mechanical measurements. On average, all unirradiated joint types exhibited torsion strengths of more than 70 MPa. The effects of neutron irradiation on the joint strength appeared insignificant for the TEP and HSiC joints, considering the statistical uncertainty. In contrast, the irradiation at low and hightemperatures degraded the joint strength of the CA joints by more than 50%. The degradation was likely due to the differential swelling between SiC and the bonding layer.

Microstructural examination of the HSiC tube-end-plug joints via XCT did not reveal any discernable microstructural changes after irradiation. Post-irradiation swelling measurements of all tube-end-plug joint specimens demonstrated linear swelling of approximately 0.45% for the lower-temperature specimens and 0.24% for the higher-temperature specimens, which is aligned with expectations based on the literature.

Following non-destructive examination, a subset of irradiated tube-end-plug joint specimens was leak tested and then destructively tested. For the CA joint specimens, three out of four were leak-tight in the low-pressure helium test but could not be tested at high pressure due to the high activity of the samples. The remaining CA joint specimen and one of the HSiC specimens exhibited leak tightness

at higher-pressure (1atm) helium. Two HSiC joint specimens showed a degradation in hermeticity following irradiation. None of the TEP samples were sufficiently leak-tight to warrant post-irradiation leak testing. Mechanical EPPO testing showed EPPO apparent burst strengths of 27–45 MPa for unirradiated HSiC tube-end-plug specimens and 19–30 MPa following irradiation. However, considering the data deviation, the results of this study do not indicate significant degradation of HSiC burst strength by irradiation.

The team developed Ansys models to simulate the three joint specimens (i.e., torsion, DNS, tubeend-plug) used in this work and each of the studied joint formulations. The model used joint-specific material properties, which were obtained by direct measurement of bulk joint material (in the case of CA and TEP) or by combining literature data and microstructural examination (HSiC). The infiltration process causes a geometrydependent density gradient in the HSiC joint, and the distance- and density-dependent properties were approximated by segmenting the joint into three regions based on the absolute distance from the outer surface of the sample.

Researchers determined the failure criteria used when simulating joint loading in the model based on experimental test results of torsion specimens for all three joint formulations. For the HSiC joint formulation, the failure criteria included an iterative process in determining a reference shear strength. The model was used to simulate DNS and EPPO mechanical performance using the failure criteria developed in this work.

In general, the model overpredicted the strength and performance of the DNS and EPPO specimens. This finding is due to the larger joint area in these specimens compared to the relatively small one in the torsion specimens used to define the failure criteria. The model reasonably predicted EPPO strengths for joints that did not require pressure for processing, agreeing with experimental data within 31% (for HSiC) and 12% (for CA joints). The team observed a larger discrepancy for the TEP joint, where the simulation significantly overpredicted the failure load.

### **Discussion**

SiC fiber reinforced SiC matrix (SiC-SiC) composites have been an attractive material option for accident-tolerant fuel cladding for LWRs and advanced reactors because of their inherent low neutron absorption, dimensional stability under high-dose neutron irradiation, and high-temperature capability. A reliable joining technology is essential for practical component applications, such as joining end plugs to seal fuel pellets inside a cladding tube. These joints cannot be a weak link in the overall safety and reliability of the fuel cladding. Thus, they must retain fission products inside the cladding and withstand irradiation and hydrothermal corrosion during regular operation. Although some joining technologies provide good strength retention after neutron irradiation at elevated temperatures, the specimen geometries (i.e., planar joints) studied in prior work were irrelevant to fuel-cladding applications. A robust, hermetic end-plug joint subjected to neutron irradiation addresses the crucial feasibility issues for deploying SiC-SiC components. The feasibility of SiC-SiC components is the primary objective of this study.

The first-of-a-kind mechanical, thermal, permeability and irradiation-performance data generated in this project have helped to identify joining methods that provide these needed characteristics for use in nuclear

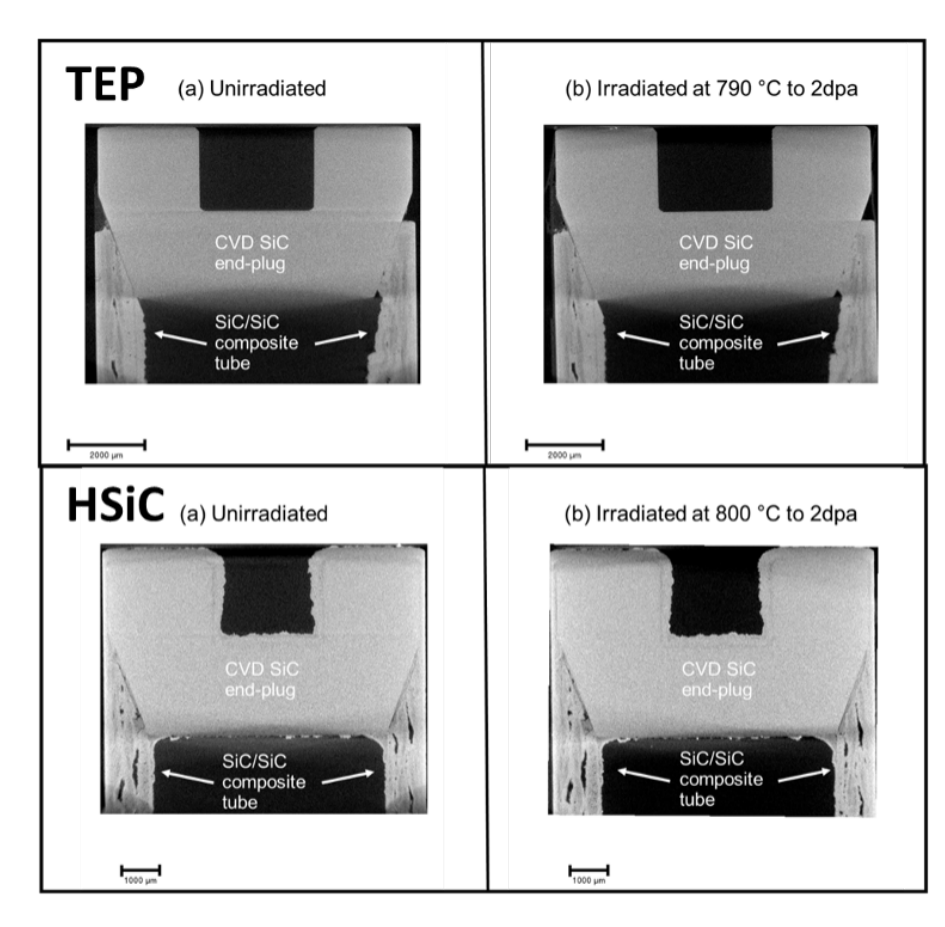


Figure 4: (top) Radiographs of TEP tube-end-plug joint: (a) unirradiated and (b) irradiated at 790°C to 2 dpa. (bottom) Radiographs of HSiC tube-end-plug joint: (a) unirradiated and (b) irradiated at 800°C to 2 dpa. No discernable microstructural changes caused by irradiation were observed.

applications in representative component geometries. While the three joint formulations selected for this project all had good attributes based on the prior literature, this current work revealed some significant challenges with forming joints in relevant geometries (tubeend-plug joints using TEP) and with specific performance characteristics (e.g., hermeticity with TEP and thermal conductivity and irradiation strength with CA joints). Of the joint types studied, the results indicate that the HSiC joining method provides good overall performance with respect to mechanical, thermal, hermetic, and irradiation resistance behaviors. This work's joint-material property data have been used to generate a material-property database to support modeling and design efforts. These data, along with the joint performance model developed in this work, can be used to achieve accelerated fuel qualification (including SiC-based cladding and joints).

The long-term impact of this work will be to help the development of advanced new materials, which can offer safer and more-efficient operation of existing and next-generation nuclear power plants in the United States. SiC-based cladding and other nuclear-reactor components provide a range of safety and operational benefits. SiC-based components can offer accident performance superior compared to conventional zirconium based alloys through their exceptional high-temperature

properties. The excellent irradiation stability and creep resistance of SiC-SiC can provide added margin to operational limits compared to conventional materials; SiC cladding can work with high-burnup, high-enrichment fuel. Along with their desirable nuclear properties (including a lower neutron-capture cross-section than zirconium alloys or steels), SiC cladding and components can offer fuelcycle cost savings and potential refueling interval extension of up to 24 months. These fuel-cycle cost savings can help make the economic case for utilities to extend the life of existing LWRs even in the current environment of strong competition from inexpensive gas and renewables. For next-generation reactors, SiC-SiC can operate in high-temperature or corrosive chemical conditions and withstand high-irradiation damage doses where zirconium or steel could not survive. This information can allow for designs, such as gas-cooled reactors, with improved electricalgeneration efficiency (obtained from high coolant temperatures) and with longer fuel life and higher burnup for more-efficient fuel utilization (enabled by the irradiation stability of SiC at high-temperatures). SiC joining and the SiC-SiC components realized by successful SiC-joining technologies are a real enabling technology for next-generation reactors to reach their true potential and support the U.S. nuclear industry from the current fleet to the next.

### **Conclusion**

Researchers investigated three promising SiC-joining methodologies (i.e., TEP, CA, and HSiC) for nuclear applications, such as fuel cladding, for current and advanced reactors. As a result, the team obtained extensive out-ofpile joint-performance data, and tube-end-plug and torsion samples were successfully irradiated in HFIR, reaching ~2 dpa neutron irradiation damage. In addition, this work obtained critical experimental data to understand the responses of SiC-SiC composite end-plug-joints to neutron irradiation. Significant accomplishments and conclusions for this project are as follows.

The HSiC joint method produced reliably strong and leak-tight joints in representative cladding geometries. Joining, mechanical, and gas-tightness results from the joints in representative cladding geometries revealed fabrication

compatibility concerns for both the TEP and CA joints. While both joints showed promising strength for cladding applications during EPPO testing, both methods had difficulty producing a reliably leaktight joint. High-temperature DNS testing of planar samples showed that the HSiC joints demonstrated excellent mechanical stability. In contrast, the CA and TEP joints exhibited variations in shear strength when tested at different temperatures, which could be a response to fabrication consistency in the sample, rather than to the fundamental joint material.

Using LFA, researchers verified a first-of-a-kind ability to measure thermal diffusivity on torsion joint-specimens. This ability shows thermal and mechanical measurements from the same set of specimens, which can effectively double the amount of data obtained from irradiated torsion-joint

specimens. Analysis of the torsionjoint sample LFA measurements also enabled the calculation of the thermal-conductivity contribution of the joint material by itself, separating this from the contribution of the monolithic CVD SiC substrate material. The thermal conductivity of the as-fabricated TEP and HSiC joints was considerably more significant than that of the CA oxide joints. TEP and HSiC saw a reduction in thermal conductivity during irradiation due to the highly crystalline SiC content in these joint compositions, compared to the amorphous oxide CA joint.

There were no statistically significant irradiation effects on the shear strength of the TEP and HSiC joints based on mechanical testing of 25 torsion joint specimens. In contrast with the TEP and HSiC, irradiation reduced the CA joint shear strength by more than 50%. Post-irradiation EPPO testing of a limited number of

HSiC joints showed no statistically significant change in joint-strength in the representative tube-endplug geometry. By contrast, the TEP joint showed significantly varying performance depending on the specimen geometry. The planar joint was robust even after neutron irradiation, as indicated by substrate failures during the torsion-test. Because of the process-induced cracking, the end plug joint showed relatively low strength and poor hermeticity. The joining process will need improvement to achieve a crack-free TEP joint with end-plug geometry.

The HSiC joint showed the best overall combination of performance characteristics (i.e., strength, thermal, hermeticity, and irradiation stability) that are desirable for nuclear fuel cladding applications. Microstructural examination of the HSiC joints via XCT does not reveal any noticeable microstructural changes after irradiation.

After irradiation in representative tube-end-plug geometries, researchers achieved the first-of-a kind demonstration of helium leak-tight joints for HSiC and CA joint-formulations. All the HSiC end-plug specimens exhibited good hermeticity in as fabricatedcondition and good strength retention after irradiation for both the end-plug and torsion samples. Although CA tube-end-plug specimens and one HSiC tube-endplug specimen remained hermetic after irradiation, the overall postirradiation hermeticity results were inconsistent, with degradation in hermeticity observed in some samples while others remained unchanged after irradiation. These results highlight the need for a better understanding of joint performance and the impact of irradiation and processing conditions.

### **Future Activities**

Several future model refinements could improve the model's accuracy as a predictive tool for SiC joint performance. In general, the model overpredicted the strengths and performance of the joint in specific simulated test configurations. The overpredictions are likely due to the larger joint area in these specimens compared to the relatively small joint area in the torsion specimens used to define the failure criteria. A size-dependent consideration may be needed in future model updates to capture this effect. Other refinements include adding a microstructure-dependent factor to better account for porosity in the joint (already implemented for HSiC joints but may be needed for the CA joints). Direct joint-tensile strength data would be beneficial for modeling more-complex stress states. Also, the current model does not account for geometry effects for joint formulations requiring pressure. In the case of a joint that requires pressure during processing, quantifying these fabrication and geometric impacts would be essential to make the model more versatile (beyond joints processed without pressure and in simpler geometries).

Researchers encountered process challenges in fabricating joints. Areas needing improvement include pressure application in the TEP joint in non-planar geometries and joint uniformity in the CA joint over larger joint areas. The HSiC joint performed well in the representative tube-endplug geometry but has limitations for joints that extend deep into a part (limited infiltration). For the future application of TEP or CA joints, modifications in fixturing or process refinements could improve the performance of these joints in specific applications.

While the thermal and mechanical results were relatively consistent, the leak rate showed wider variability after irradiation. There was a broader range in measured leak values for the CA joints, and improvements in process repeatability would be beneficial to obtain a larger yield of leak-tight joint samples (ideally approaching the 100% as-fabricated yield from HSiC samples in this work). The post-irradiation confirmation of leak tightness in one CA and one HSiC joint was a significant result; however, other CA and HSiC joints lost hermeticity following irradiation. A better understanding of these effects and causes is needed to have

a more reliable joint formulation regarding retention of gas tightness.

More broadly, this research contributes to an overall goal to develop, demonstrate, and license SiC-based, accident-tolerant fuel cladding for deployment in current LWRs and future advanced-reactor applications. This work is one part of a comprehensive effort spanning multiple projects. Parallel and ongoing work could include the demonstration of robust scalable manufacturing methods for cladding and end plug joints; obtaining irradiation performance verification of subscale fueled rodlets in increasingly representative conditions; validation of a digitaltwin cladding model to support accelerated fuel qualification; and future material, lead test rod, and lead test assembly irradiations in commercial reactors to gather data to support Nuclear Regulatory Commission licensing. This work will enable the U.S. nuclear industry to benefit from the exceptional properties and capabilities of SiC ceramic matrix composite components to improve reactor safety, economics, and performance.

### References

- [1.] ASTM C1862-17. 2017. "Standard Test Method for the Nominal Joint Strength of End-Plug Joints in Advanced Ceramic Tubes at Ambient and Elevated Temperatures."

  ASTM International, West Conshohocken, PA, 2017, www. astm.org.
- [2.] ASTM C1469-10. 2015. "Standard Test Method for Shear Strength of Joints of Advanced Ceramics at Ambient Temperature."

  ASTM International, West Conshohocken, PA, 2015, www. astm.org.
- [3.] ASTM Standard E1461–13. 2013. "Standard Test Method for Thermal Diffusivity by the Flash Method." ASTM International, West Conshohocken, PA, 2013, www.astm.org.
- [4.] Campbell, A., et al. 2016.

  "Method for Analyzing Passive
  Silicon Carbide Thermometry
  with a Continuous Dilatometer
  to Determine Irradiation
  Temperature." Nuclear
  Instruments and Methods in
  Physics Research B 370: 49–58.
- [5.] Jacobsen, G. M., et al. 2015., "High-temperature Testing of Geometrically Relevant, Nuclear Grade, Silicon Carbide Joints. "Trans of the American Nuclear Society, 113: 535–538.
- [6.] Jacobsen, G. M., and H. Chiger. 2017. "Product Engineering Materials Property Manual:

- General Atomics Silicon Carbide Cladding, Revision 1." General Atomics Project #30446, October 2017.
- [7.] Katoh, Y., et al. 2014. "Radiation-Tolerant Joining Technologies for Silicon Carbide Ceramics and Composites." Journal of Nuclear Materials 448, no. 1-3 (May): 497–511.
- [8.] Katoh, Y., et al. 2000.

  "Microstructure and Mechanical Properties of Low-Activation Glass-Ceramic Joining and Coating for SiC/SiC Composites."

  Journal of Nuclear Materials 283: 1262–1266.
- [9.] Khalifa, H. E., et al. 2015. "Fabrication and Characterization of Joined Silicon Carbide Cylindrical Components for Nuclear Applications." Journal of Nuclear Materials 457: 227– 240.
- [10.] Khalifa, H. E., et al. 2017.

  "Radiation Stable, Hybrid,
  Chemical Vapor Infiltration/
  Preceramic Polymer Joining of
  Silicon Carbide Components."
  Journal of Nuclear Materials
  487: 91–95.
- [11.] Kim, J. G., et al. 2017.

  "Evaluation of the CrossPlane Thermal Conductivity
  of Double-Layer Materials."

  Composites Part B: Engineering
  110: 1–6. Koyanagi, T., et al.
  2017.

- [12.] "Irradiation Resistance of Silicon Carbide Joint at Light Water Reactor-Relevant Temperature." J. Nucl. Mater. 488: 150–159. https://doi.org/10.1016/j. jnucmat.2017.03.017.
- [13.] McDuffee, J. L., 2011. "Heat Transfer Coefficients and Bulk Temperatures for HFIR Rabbit Facilities." DAC-11-01-RAB03, Rev. 0, Oak Ridge National Laboratory, Thermal Hydraulics, and Irradiation Engineering Group.
- [14.] Petrie, C. M., et al. 2017.

  "Experimental Design and Analysis for Irradiation of SiC/SiC Composite Tubes under a Prototypic High Heat Flux." Journal of Nuclear Materials 491: 94–104, https://doi.org/10.1016/j. jnucmat.2017.04.058.
- [15.] Petrie C. M., and T. Koyanagi. 2017. "Assembly and Delivery of Rabbit Capsules for Irradiation of Silicon Carbide Cladding Tube Specimens in the High Flux Isotope Reactor." ORNL/TM-2017/433, Oak Ridge National Laboratory.

### **Publications:**

- [1.] Koyanagi, T., et al. 2022. "Endplug and Torsion Specimen Post-Irradiation Examination." ORNL/ SPR-2022-2510, Oak Ridge National Laboratory.
- [2.] Gonderman, S. 2018. "Technical Report on Specimen Geometries Selected for Characterization and Irradiation Design Needs."
  General Atomics Project Report #GA-C28913, General Atomics Project #30494, July 2018.
- [3.] Petrie, C.M., et al. 2018. "Design and Thermal Analysis for Irradiation of Silicon Carbide Joint Specimens in the High Flux Isotope Reactor." ORNL/ TM-2018/940, Oak Ridge National Laboratory, 2018.
- [4.] Le Coq, A. G., et al. 2019.

  "Assembly of Capsules for Irradiation of Silicon Carbide Joint Specimens in the High Flux Isotope Reactor." ORNL/SPR-2019/1392, Oak Ridge National Laboratory, 2019.
- [5.] Gonderman, S., and C. P. Deck.
  2019 "Technical Report on
  Out-of-Pile Mechanical,
  Thermal, and Microstructural
  Characterization." General
  Atomics Project Report #GAC28761, General Atomics
  Project #30494, December 2019.

- [6.] Werden, J., et al. 2020.
  "Disassembly of Capsules after Irradiation of Silicon Carbide Joint Specimens in the High Flux Isotope Reactor." ORNL/SPR-2020/1841, Oak Ridge National Laboratory, 2020.
- [7.] Deck, C. P., 2021"Modeling the Mechanical Response of Joints for SiC-SiC Components." General Atomics Project Report #GA-C29607, General Atomics Project #30494, September 2021.
- [8.] Koyanagi, T., and J. A. Mena. 2021. "Post-Irradiation Examinations of Neutron-Irradiated SiC Joints." ORNL/SPR-2021/2277, Oak Ridge National Laboratory, 2021.

- [9.] Deck, C. P., 2021 "Analysis of Joints for Silicon Carbide Components After Irradiation." General Atomics Project Report #30494R00001, General Atomics Project #30494, September 2021.
- [10.] Deck, C. P., 2021 "Final Technical Report: Performance of SiC-SiC Cladding and End Plug Joints under Neutron Irradiation with a Thermal Gradient." General Atomics Project Report #GA-C29635, General Atomics Project #30494, September 2021.

Distributed Partnership at a Glance		
NSUF Institution	Facilities and Capabilities	
Oak Ridge National Laboratory	High-Flux Isotope Reactor Irradiated Materials Examination and Testing Facility Hot Cells Low Activation Materials Design and Analysis Laboratory	
Collaborators		
General Atomics	Christian Deck (Co-Principal Investigator)	
General Atomics	Sean Gonderman (Team Member), Herb Shatoff (Team Member)	
Oak Ridge National Laboratory	Takaaki Koyanagi (Co-Principal Investigator)	
Oak Ridge National Laboratory	Christian Petrie (Team Member)	

### Understanding Swelling Related Embrittlement of AISI 316 Stainless Steel Irradiated in EBR-II

Cheng Sun - Idaho National Laboratory - cheng.sun@inl.gov



eutron irradiation causes degradation of the mechanical properties of materials due to the formation of irradiation defects that can change the deformation mechanisms. Many years of experimental and modeling efforts on irradiation damage and effects have generated a substantial knowledge database on the evolution of microstructure. microchemistry, and mechanical properties of materials under lowdose neutron irradiation. However, due to the limited database of highdose neutron-irradiation studies, a complete understanding remains unclear concerning microstructural evolution and corresponding mechanical property changes under high-dose neutron irradiation. This project investigated swellinginduced embrittlement of American Iron and Steel Institute (AISI) 316 SS irradiated in Experimental Breeder Reactor II, a sodium-cooled fast reactor. The research team examined the microstructure, microchemistry, and mechanical properties of high-dose, neutron-irradiated AISI

316 SS. They observed a strong correlation between elongation after yielding and void swelling. The role of void swelling on the deformation mechanisms was made clear. Understanding the mechanical behaviors of high-dose, neutron-irradiated core internals is vital to developing advanced materials for the next generation of nuclear reactors.

#### Introduction

Austenitic AISI 316 SS has been widely used for the structural components in LWRs and proposed as critical structural materials for the next generation of nuclear reactors due to their excellent mechanical properties. However, irradiationinduced defects and precipitation could lead to hardening and embrittlement. At low irradiation temperatures (<360°C) and low irradiation doses (<10 dpa), neutron irradiation typically creates black dots and dislocation loops in 316 SS. The interaction between mobile dislocations and dislocation loops causes dislocation channeling, a

localized deformation mode. At higher irradiation temperatures and higher irradiation doses, irradiationinduced voids could cause severe embrittlement. Some studies have shown that AISI 316 SS could lose ductility when swelling reaches 10 percent. Such severe embrittlement arises from the intense deformation localization and void-to-void cracking. Despite the efforts, a direct correlation between microstructure. chemical redistribution, and mechanical properties is still missing, and the effect of void swelling on deformation mechanisms remains unclear.

### **Project Hypothesis**

Neutron irradiation of austenitic 316 is known to cause embrittlement. However, the deformation mechanism of 316 SS after high-dose neutron irradiation remains unclear. In this project, the research team studied the microstructure and microchemistry of 316 SS irradiated in a fast reactor to high neutron fluences and the influence of void swelling on the deformation mechanisms.

Understanding the deformation mechanism of high dose, fast neutron irradiated materials is essential for the development of advanced structural materials for advanced reactors.

## **Experimental or Technical Approach**

Researchers used transmission electron microscopy (TEM), atomprobe tomography, and ring tensile testing.

### **Results**

The research team performed TEM characterizations of the irradiated 316 SS specimens. A high density of voids and precipitates formed at each irradiation condition. The team measured void size and void density to calculate volumetric swelling. They performed chemical analysis of irradiated specimens using energy-dispersive spectroscopy (EDS) equipped on Titan Themis. Researchers observed Ni-Si precipitates with an average diameter of ~10 nm, which had formed in the matrix close to the voids, and enrichment of Ni, Si, and P near the voids. The chemical segregation near the voids leads to the changes in sink strength to irradiation defects and furthers the embrittlement of the specimens. Fe, Cr, Mn, and Mo are depleted along grain boundaries, while Ni and Si are enriched along the grain boundary. The dark-field scanning transmission electron microscope (STEM) image also reveals a void-denuded zone near the grain boundary. The formation of voids and chemical redistribution (e.g., precipitation, chemical segregation on voids, and grain boundaries) cause severe changes in the mechanical properties of the irradiated specimens.

The research team characterized the fractography of deformed specimens using a scanning electron microscope (SEM). The fracture surface of the reference sample mainly has dimple-like morphologies, suggesting a ductile failure of materials. With increasing swelling from 1.8–13.33%, the dimple-like failure gradually becomes cleavage failure, which is depicted by a river pattern in SEM images. Cleavage fracture results in embrittlement. Fractography

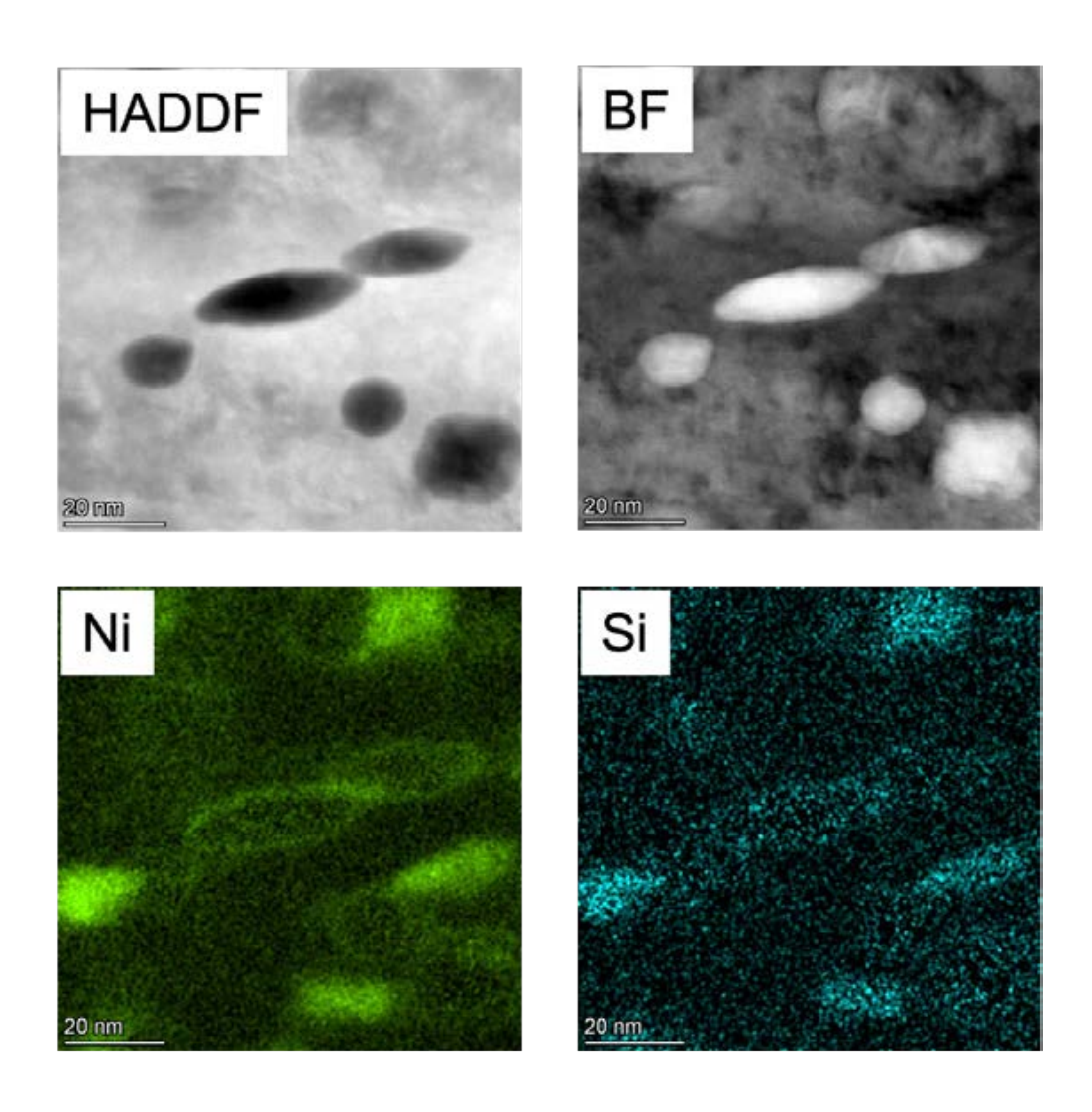


Figure 1. Microstructure and microchemistry of high dose, fast neutron irradiated 316L SS after tension test.

examination is consistent with the ring tensile tests of irradiated specimens; i.e., the elongation-tofailure decreases from ~75 to 5%. Although the irradiated specimen became brittle, an enlarged SEM micrograph shows band structures in the grain interiors. TEM characterization in the next section reveals that these band structures are deformation-induced twins. Researchers examined the chemical analysis of deformed reference and irradiated specimens using EDS and wavelength-dispersive spectroscopy. The EDS mapping of Fe, Cr, Ni, Mn, Mo, and Si indicates the marked region in the SEM image. There was no clear evidence of chemical variations within the dimple features in the deformed reference sample. Researchers prepared TEM lamellae from the deformed region of the tested ring specimens. Microstructure and chemical analysis were performed for the eight specimens (one reference and seven irradiated specimens) through TEM and EDS. TEM micrographs reveal that deformation twinning is predominant in the irradiated specimen. EDS mapping of the deformed irradiated specimen shows that the previous spherical voids become elongated along the twin interfaces. In addition, the Ni-Si

enriched precipitates were sheared and became elongated along twin interfaces. Voids with Ni and Si enrichment are also sheared in the twin domain and become elongated.

### **Discussion:**

Understanding the deformation mechanisms of fast-neutronirradiated alloys is essential to developing novel structural materials for fast nuclear reactors. This research provides new insights into the swelling-induced embrittlement in austenitic 316 SS subjected to high-dose, fast-neutron irradiation. PIE reveals a high density of voids, decorated by Ni and Si phase formed in the microstructure. Voids provide a strong strength barrier for dislocation movement. During tensile tests at room temperature, deformation twinning is the predominant deformation mechanism in irradiated 316 SS at high swelling levels. The interaction of twins and voids causes void elongation, shrinkage, and linkage, leading to localized deformation. The fundamental understanding gained in this project provides a scientific basis for developing irradiation tolerant materials for fast reactors.

### **Conclusion:**

In this project, the team characterized the microstructure and microchemistry of high-dose, neutron-irradiated AISI 316 SS. Researchers identified irradiationinduced void swelling and chemical redistribution (i.e., chemical segregation near voids, grain boundaries, and precipitation). The high density of voids and Ni-Si precipitates formed in the grain interiors, and voids are decorated with the Ni-Si phase. Ring hoop tensile testing showed that elongation after yielding strongly depends on the void swelling. The fractography of fracture surfaces revealed that the dimple-like failure mode gradually turns to cleavage failure mode as the swelling increases, suggesting the vital role of void swelling in the deformation mechanisms. Deformation twinning is predominant in the irradiated specimens during the tension test at room temperature. The shearing of Ni- and Si-enriched voids and precipitation during twinning could further cause the hardening and embrittlement. This work provides new insights into the deformation behavior of fast-neutron-irradiated SS and can be applied to design and synthesize novel materials for advanced nuclear systems.

### **Future Activities:**

Further understanding of deformation mechanism at high dose by atomistic modeling and simulation.

### References

- [1.] Sun, C., et al. 2015. "Superior Radiation-Resistant Nanoengineered Austenitic 304L Stainless Steel for Applications in Extreme Radiation Environments." Sci. Rep. 5: 7801. https://doi. org/10.1038/srep07801.
- [2.] Sencer, B. H., et al. 2003. "Proton Irradiation Emulation of PWR Neutron Damage Microstructures in Solution Annealed 304 and Cold-Worked 316 Stainless Steels." J. Nucl. Mater. 323: 18–28. https://doi.org/https://doi.org/10.1016/j.jnucmat.2003.07.007.
- [3.] Rabenberg, E. M. 2014.

  "Mechanical behavior of
  AISI 304SS Determined by
  Miniature Test Methods
  after Neutron Irradiation to
  28 dpa." J. Nucl. Mater. 448:
  315–324. https://doi.org/
  https://doi.org/10.1016/j.
  inucmat.2014.02.018.

- [4.] Bond, G. M., et al. 1999. "Void Swelling of Annealed 304 Stainless Steel at ~370–385°C and PWR-Relevant Displacement Rates." Ninth Int. Symp. Environ. Degrad. Mater. Nucl. Power Syst. React., Wiley Online Library, 1999: 1045–1050.
- [5.] E. Wood, and F. Garner.,
  F. 1990. "Influence of
  Thermomechanical Treatment
  and Environmental History
  on Creep, Swelling, and
  Embrittlement of AISI 316
  at 400 Cand 130 dpa." Eff.
  Radiat. Mater. 14th Int.
  Symp. (Volume II), ASTM
  International, 1990.
- [6.] Porollo, S.I., et al. 1998.

  "Swelling and Void-Induced
  Embrittlement of Austenitic
  Stainless Steel Irradiated to
  73–82 dpa at 335–365°C." J.
  Nucl. Mater. 258: 1613–1617.
- [7.] Neustroev, V.S., and F.A. Garner, 2009. "Severe Embrittlement of Neutron Irradiated Austenitic Steels Arising from High Void Swelling." J. Nucl. Mater. 386: 157–160.

### **Publications**

Two manuscripts in preparation.

Distributed Partnership at a Glance			
NSUF Institution	Facilities and Capabilities		
Idaho National Laboratory	Electron Microscopy Laboratory Hot Fuel Examination Facility Irradiated Materials Characterization Laboratory		
Westinghouse Electric Company	Churchill Laboratory Services		
Collaborators			
Idaho National Laboratory	Cheng Sun (Principal Investigator), Douglas L. Porter (Co-Principal Investigator), Wen Jiang, (Co-Principal Investigator)		
Idaho National Laboratory	Boopathy Kombaiah (Team Member), Mukesh N. Bachhav(Team Member)		
Texas A&M University	Frank Garner (Co-Principal Investigator)		
Westinghouse Electric Company	Michael Ickes (Team Member)		

### SHORT COMMUNICATIONS

### ChemiSTEM Characterization of Bulk Heavy Ion-Irradiated Complex Concentrated Alloys

Calvin Parkin - University of Wisconsin-Madison - cparkin@wisc.edu, caparki@sandia.gov



onventional nuclear structural alloys show dramatic degradation after hundreds of displacements per atom, which inadequately meet the needs of advanced reactors, triggering exploration of CCAs. Preliminary studies demonstrate the excellent strength, high-temperature performance, and irradiation tolerance of CCA, promoting their candidacy for cladding and duct applications [1-20]. To advance fundamental understanding of the radiation resistance of compositionally complex base matrices, high-temperature irradiations were performed on  $Cr_{18}Fe_{27}Mn_{27}Ni_{28}$  and  $Cr_{15}Fe_{35}Mn_{15}Ni_{35}$ to high dpa. STEM and super-X were used to characterize the microstructural evolution in terms of defects and chemical segregation.

### **Experimental or Technical Approach**

To investigate the effect of high dose on microstructural evolution,  $Cr_{18}Fe_{27}Mn_{27}Ni_{28}$  and  $Cr_{15}Fe_{35}Mn_{15}Ni_{35}$ were irradiated at 500°C at the Texas A&M University Accelerator Laboratory using a defocused beam of 5.0 MeV Ni<sup>2+</sup> ions up to 50, 100, and 200 dpa at the midrange of the plateau region of the damaged profile as computed by the Stopping and Range of lons in Matter (SRIM) code [21]. Alloy selection, fabrication, preparation, precharacterization, and SRIM inputs are detailed in the references [11] and [3]. Displacement damage and implanted-ion profiles for Cr<sub>18</sub>Fe<sub>27</sub>Mn<sub>27</sub>Ni<sub>28</sub> are shown in Figure 1. TEM lamellae were extracted using focused ion beam and were examined using a Titan Themis 200 and Thermo Scientific Talos F200X TEMs with EDS systems at the Irradiated Materials Characterization Laboratory and Electron Microscopy Laboratory facilities at Idaho National Laboratory to characterize radiation-induced segregation and void swelling. Voids were measured by hand using ImageJ

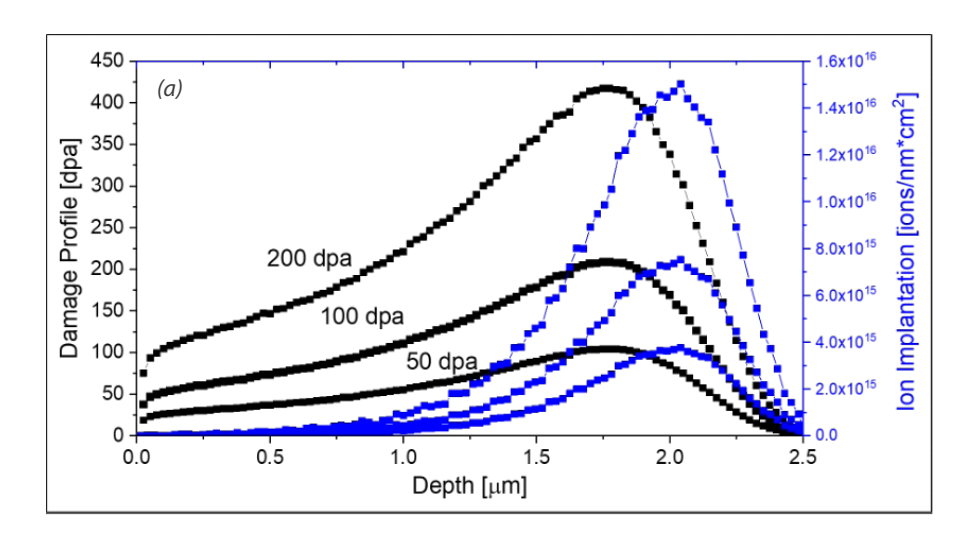


Figure 1. Dpa and ion-implantation profiles for  $Cr_{18}Fe_{27}Mn_{27}Ni_{28}$  generated by SRIM for 5.0 MeV  $Ni^2+$  ions at 50, 100, and 200 dpa.

software and using random forest regression image processing software IPSDK by Reactiv'IP [22]. EDS quantifications were performed using the Thermo Scientific Velox software with the default Brown-Powell ionization cross-section model and multipolynomial model for background correction. Lamellae thicknesses were measured by a direct electron method (K2 camera) and a slit width of 15 eV.

### Results

All irradiations except  $Cr_{15}Fe_{35}Mn_{15}Ni_{35}$  to 50 dpa resulted in void growth, faulted interstitial loops, and chemical redistribution. An example is shown in Figure 2 of a micrograph of  $Cr_{15}Fe_{35}Mn_{15}Ni_{35}$  irradiated to 100 dpa, EDS line scans through the irradiated depth and near a void, and chemical maps near a void. The mapping for each depth profile is analyzed and averaged over several microns.

EDS profiles are smoothed using an adjacent averaging function. A larger diffuse border of the void in the Mn map indicates vacancies have exchanged more favorably with Mn than with Fe or Cr. The Mn enrichment and Ni depletion just before the displacement peak in the depth profile is consistent across all irradiations except Cr<sub>15</sub>Fe<sub>35</sub>Mn<sub>15</sub>Ni<sub>35</sub> to 50 dpa and with the irradiations in reference [3]. Swelling levels, as measured manually and by IPSDK, are indicated in Figure 3, which agreed well. Cr<sub>15</sub>Fe<sub>35</sub>Mn<sub>15</sub>Ni<sub>35</sub> swelled less than Cr<sub>18</sub>Fe<sub>27</sub>Mn<sub>27</sub>Ni<sub>28</sub> with increasing dosage and experienced less redistribution of Mn with depth. All EDS results indicate Ni becomes enriched near the periphery of voids. A relrod contrast revealed a population of faulted dislocation loops (Figure 4). The average diameter, number density, and dislocation line density are shown in Table 1.

Table 1. Average faulted loop diameter, loop number density, and dislocation density in CCAs irradiated to 50, 100, and 200 dpa at 500°C. [14].

				Loop Diameter [nm] Number Density [m-3]		Dislocation Line Density [cm <sup>-2</sup> ]			
dpa	50	100	200	50	100	200	50	100	200
Cr <sub>18</sub> Fe <sub>27</sub> Mn <sub>27</sub> Ni <sub>28</sub>	11 ± 6	3 ± 2	6 ± 3	$4.83 \times 10^{21}$	$1.27 \times 10^{23}$	$5.57 \times 10^{22}$	1.69 × 10 <sup>10</sup>	1.37 × 10 <sup>11</sup>	9.84 × 10 <sup>10</sup>
Cr <sub>15</sub> Fe <sub>35</sub> Mn <sub>15</sub> Ni <sub>35</sub>	11 ± 5	5 ± 2	7 ± 3	$2.0 \times 10^{21}$	3.74 × 10 <sup>22</sup>	1.01 × 10 <sup>22</sup>	$2.76 \times 10^{10}$	5.6 × 10 <sup>10</sup>	2.31 × 10 <sup>10</sup>

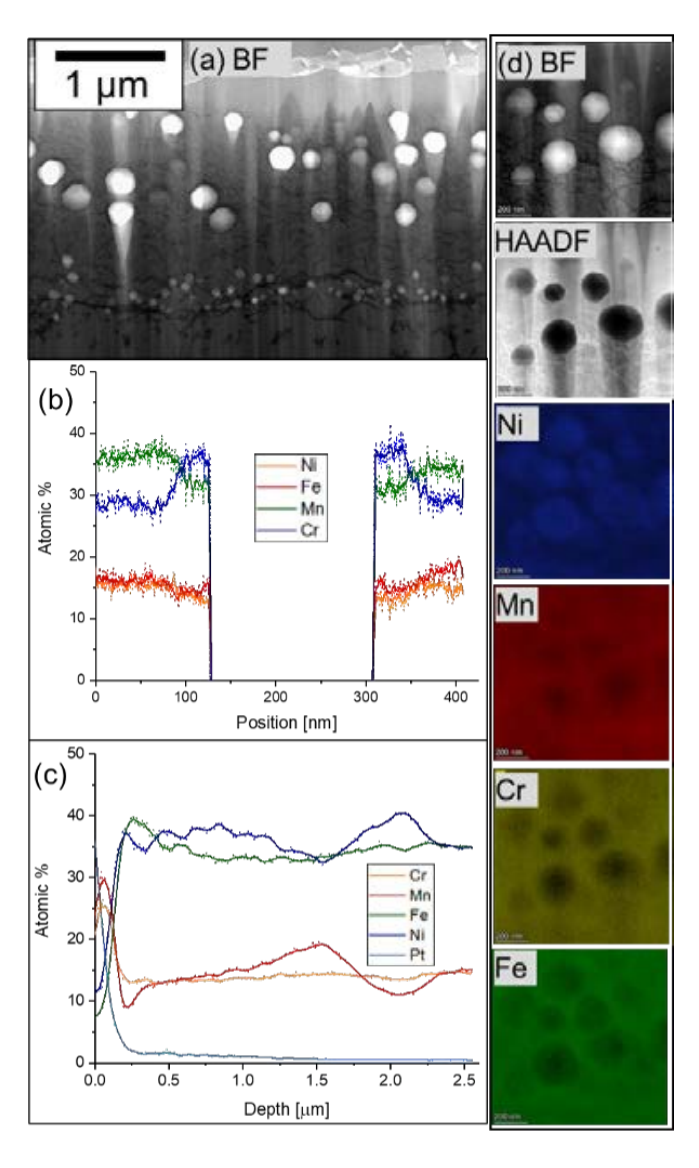


Figure 2. (a) Slightly underfocused micrograph of voids in  $Cr_{15}Fe_{35}Mn_{15}Ni_{35}$  irradiated to 100 dpa at 500°C. (b) Super-X EDS linescan across void. (c) Super-X EDS line scan through irradiation depth. (d) Bright-field, HAADF, and super-X EDS maps showing Ni enrichment.

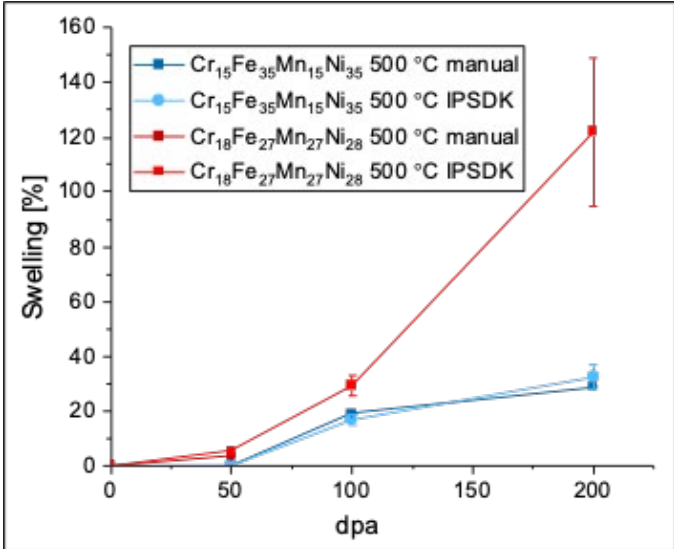


Figure 3. Swelling levels from irradiations comparing manual void measurement to IPSDK software measurement and  $Cr_{18}Fe_{27}Mn_{27}Ni_{28}$  to  $Cr_{15}Fe_{35}Mn_{15}Ni_{35}$ .

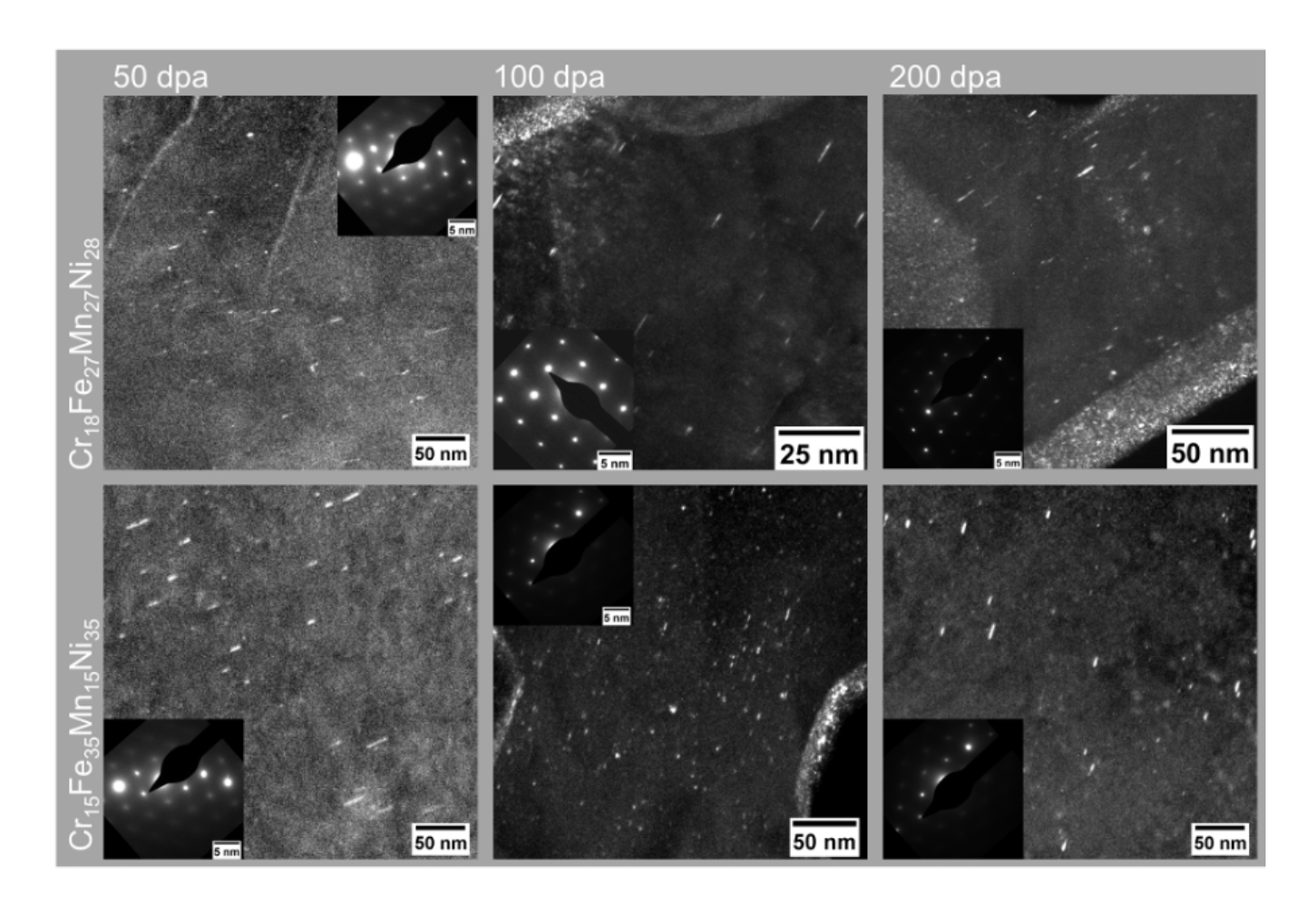


Figure 4. Faulted loops observed in  $Cr_{18}Fe_{27}Mn_{27}Ni_{28}$  and  $Cr_{15}Fe_{35}Mn_{15}Ni_{35}$  at 50, 100, and 200 dpa.

### **Discussion/Conclusion**

Void nucleation, growth, and chemical redistribution in  $Cr_{18}Fe_{27}Mn_{27}Ni_{28}$  and  $Cr_{15}Fe_{35}Mn_{15}Ni_{35}$  at various dpa were consistent with the 75 dpa irradiations in reference [3]. Depth-dependent Mn redistribution indicates that vacancies diffuse preferentially via Mn-exchange. Ni exhibits the opposite behavior, effectively diffusing alongside vacancies and enriching the area around voids. Ni enrichment near voids has been

observed previously in reference [23], which also has reported Mn depletion near voids and attributed some swelling differences to vacancy mobility. By tailoring the Mncontent, the vacancy mobility can be tuned to prolong void nucleation and promote void-swelling resistance of the base matrix in future alloy design endeavors.

### References

- [1.] Miracle, D., and O. Senkov. 2017.
  "A Critical Review of High
  Entropy Alloys and Related
  Concepts." Acta Materialia 122:
  448–511.
- [2.] Kumar, N.A.P.K., et al. 2016.

  "Microstructural Stability
  and Mechanical Behavior of
  FeNiMnCr High Entropy Alloy
  under Ion Irradiation." Acta
  Materialia 113: 230–244.
- [3.] Parkin, C., et al. 2022. "Phase Stability, Mechanical Properties, and Ion Irradiation Effects in Face-Centered Cubic FeCrMnNi Compositionally Complex Solid-Solution Alloys at High Temperatures." Journal of Nuclear Materials 565: 153733.
- [4.] Egami, T. et al. 2013. "Irradiation Resistance of Multicomponent Alloys." Metallurgical and Materials Transactions A 45: 180–183.
- [5.] Jin, K., et al. 2016. "Effects of Compositional Complexity on the lon-Irradiation Induced Swelling and Hardening in Ni-Containing Equiatomic Alloys." Scripta Materialia 119: 65–70.

- [6.] Yang, T., et al. 2018. "Irradiation Responses and Defect Behavior of Single-Phase Concentrated Solid Solution Alloys." Journal of Materials Research 33 (19): 3077–3091.
- [7.] Lu, C., et al. 2016. "Enhancing Radiation Tolerance by Controlling Defect Mobility and Migration Pathways in Multicomponent Single-Phase Alloys." Nature Communications 7: 13564.
- [8.] Lu, C., et al. 2017. "Radiation-Induced Segregation on Defect Clusters in Single-Phase Concentrated Solid-Solution Alloys." Acta Materialia 127: 98–107.
- [9.] Jin, K. and H. Bei. 2018. "Single-Phase Concentrated Solid-Solution Alloys: Bridging Intrinsic Transport Properties and Irradiation Resistance." Frontiers in Materials 5 (26).
- [10.] Shi, S., et al. 2018. Evolution of lon Damage at 773K in Ni- Containing Concentrated Solid-Solution Alloys." Journal of Nuclear Materials 501: 132–142.

- [11.] Parkin, C., et al. 2020. "In-Situ Microstructural Evolution in Face-Centered and Body-Centered Cubic Complex Concentrated Solid-Solution Alloys under Heavy Ion Irradiation." Acta Materialia 198: 85–99.
- [12.] Chen, W.-Y., et al. 2018.

  "Irradiation Effects in High
  Entropy Alloys and 316H
  Stainless Steel at 300°C."

  Journal of Nuclear Materials
  510: 421–430.
- [13.] Li, C., et al. 2019. "Neutron Irradiation Response of a Co-Free High Entropy Alloy." Journal of Nuclear Materials 5127: 151838.
- [14.] Egami, T. 2015. "Local Electronic Effects and Irradiation Resistance in High-Entropy Alloys." The Journal of The Minerals, Metals & Materials Society 67 (10): 2345–2349.
- [15.] Körmann, F., et al. 2017. "Phonon Broadening in High Entropy Alloys." npj Computational Materials Science 3: 36.

- [16.] Zhang, Y., et al. 2016. "Influence of Chemical Disorder on Energy Dissipation and Defect Evolution in Advanced Alloys."
  Journal of Materials Research 31 (16): 2363–2375.
- [17.] Zhao, S. et al. 2019. "Frenkel Defect Recombination in Ni and Ni-Containing Concentrated Solid-Solution Alloys." Acta Materialia 173: 184–194.
- [18.] Caro, M., et al. 2015. "Lattice Thermal Conductivity of Multi-Component Alloys." Journal of Alloys and Compounds 648: 408–413.
- [19.] Béland, L., Y. Osetsky, and R. Stoller. 2016. "The Effect of Alloying Nickel with Iron on the Supersonic Ballistic Stage of High Energy Displacement Cascades." Acta Materialia 116: 136–142.
- [20.] Zhang, Y., et al. 2015. "Influence of Chemical Disorder on Energy Dissipation and Defect Evolution in Concentrated Solid Solution Alloys." Nature Communications 6: 8736.

- [21.] Stoller, R., et al. 2019. "Erratum to 'On the use of SRIM for computing radiation damage exposure [Nucl. Instrum. Methods Phys. Res. B 310 (2013) 75–80]." Nuclear Instruments and Methods in Physics Research B 459: 196–197.
- [22.] Reactiv'IP Smart Image Processing. 2022. "Image Processing." Accessed February 2023. https:// www.reactivip.com/imageprocessing/.
- [23.] Wang, X., et al. 2022. "Understanding Effects of

Chemical Complexity on Helium Bubble Formation in Ni-Based Concentrated Solid Solution Alloys Based on Elemental Segregation Measurements." Journal of Nuclear Materials 569: 153902.

### **Publications:**

[1.] Parkin, C., et al. (submission pending). "Dose and Temperature Effect in CrFeMnNi Compositionally Complex Solid-Solution Alloys under Heavy Ion Irradiation."

Journal of Nuclear Materials.

Distributed Partnership at a Glance			
NSUF Institution	Facilities and Capabilities		
Idaho National Laboratory	Electron Microscopy Laboratory Irradiated Materials Characterization Laboratory		
Texas A&M University	Accelerator Laboratory		
Collaborators			
Idaho National Laboratory	Lingfeng He (Co-Principal Investigator)		
University of Wisconsin-Madison	Adrien Couet (Co-Principal Investigator)		
Degrees Granted			
University of Wisconsin-Madison	Calvin Parkin, Ph.D.		

### Alumina-Stabilized Coatings under Irradiations: Towards Future Generation Nuclear Systems

Fabio Di Fonzo - Italian Institute of Technology - fabio.difonzo@iit.it



lumina (Al<sub>2</sub>O<sub>3</sub>) coatings produced by pulsed laser deposition (PLD) represent one of the major candidate solutions as anti-corrosion and anti-permeation for next-generation nuclear reactors [1-6]. Despite the results gathered so far, implementation in real nuclear systems requires complete knowledge of their radiation effects.

For this reason, the dynamic evolution of the radiation-induced crystallization (RIC) of thin films of amorphous Al<sub>2</sub>O<sub>3</sub> and doped Al<sub>2</sub>O<sub>3</sub> over an extensive range of temperatures was studied. The aim of the experiments was to elucidate the dependence of grain growth on ion dose, temperature, and ion type. Specifically, the team wanted to understand the synergistic effects of ion irradiation and temperature on the evolution of the amorphous microstructure, which cannot be probed through traditional PIE. The effect of doping as an RIC slowing down strategy was also investigated.

### **Experimental or Technical Approach**

The samples were fabricated by PLD. Freestanding films with a nominal thickness of 100 nm were grown on monocrystalline substrates obtained by cleaving a NaCl crystal. After deposition, each sample was put in warm distilled water where the salt dissolved, and the oxide film floated on the water's surface. Grids were used to pick up the films ready for analysis by TEM Additional information about this floating technique is included in the references [4]. The PLD-deposited alumina films were subjected to thermal heating until thermal stabilization at different temperatures (from 300-800°C). Then the films were irradiated using 700 KeV Kr ions with a flux of 6.25 10<sup>11</sup> ions/cm<sup>2</sup>s as a surrogate of neutron irradiation.

During the various *in situ* irradiation experiments, selected-area electron diffraction (SAED) patterns were recoded to precisely identify crystallization onset. For each pattern, the diameter of the ring was measured, determining the

crystalline phases in the system by directly comparing the interplanar distances obtained with the databases in the literature [7-8]. The average grain-size evolution was studied and measured from darkfield images at the different fluences for the first appearing reflection in SAED. A thresholding procedure exploiting bright field images was developed to obtain qualitative trends for the amorphous fraction evolutions at different temperatures.

#### **Results**

The RIC kinetics were obtained for pure and doped amorphous alumina thin films. The presence of yttria as a doping element reduced the crystallization kinetic, with smaller crystalline grains on average than the undoped case. This retarding effect was confirmed by the SAED-patterns observation, which was also helpful for the RIC onset determination at different temperatures.

A clear temperature dependence of the RIC for all situations was observed, confirming an Arrheniustype behavior of the crystallization kinetic. The relation between the dpa level at which RIC initiates and temperature was investigated. A power law represents the relationship between these two parameters, with a negative exponent larger than four. Due to this exponent, the extrapolation of this trend toward lower temperatures would suggest that, at room temperature, a practically infinite dose is required to induce crystallization. This is consistent with the recent observation of no crystallization hints, even at 25 dpa at room temperature [9] and supports the indication of amorphous alumina as a radiation-tolerant coating. The presence of doping also had a beneficial effect in this case, showing that higher radiation doses are needed to induce the crystallization than in the undoped case at the same temperature.

### **Discussion/Conclusion**

This study enhanced the knowledge on amorphous  $Al_2O_3$  produced by PLD, providing key insights for their use as protective coatings in next-generation reactors' radiation rich environments. The interplay was studied between radiation

dose, temperature, and doping on the crystallization kinetics of amorphous Al<sub>2</sub>O<sub>3</sub>. The data gathered over a wide range of temperatures enabled the team to verify that the model chosen to describe the crystallization was valuable, at least for the dose levels analysed. An accurate understanding of phase evolution at different temperatures was obtained from SAED's intensity profiles investigation. Hints on control strategies on the RIC of PLD a-Al<sub>2</sub>O<sub>3</sub> were gathered, paving the way to a future generation of radiation-resistant coatings for GIV and fusion environments.

### References

- [1.] Ferré, F. García, et al. 2013.

  "Advanced Al2O3 coatings for
  High Temperature Operation
  of Steels in Heavy Liquid
  Metals: A Preliminary Study."
  Corrosion Science 77: 375–
  378.
- [2.] Ferré, F. García, et al. 2017.

  "Corrosion and Radiation
  Resistant Nanoceramic
  Coatings for Lead Fast
  Reactors." Corrosion Science
  124: 80–92.
- [3.] Iadicicco, D., et al. 2019.

  "Multifunctional Nanoceramic
  Coatings for Future
  Generation Nuclear Systems."
  Fusion Engineering and
  Design 146: 1628–1632.
- [4.] Frankberg, Erkka J., et al. "Highly Ductile Amorphous Oxide at Room Temperature and High Strain Rate." Science 366(6467): 864–869.

- [5.] Utili, Marco, et al. 2022. "Design of the Test Section for the Experimental Validation of Antipermeation and Corrosion Barriers for WCLL BB." Applied Sciences 12(3): 1624.
- [6.] Zaborowska, A., et al. "Absolute Radiation Tolerance of Amorphous Alumina Coatings at Room Temperature." Ceramics International (47)24 34740–34750.
- [7.] Souza Santos, P., H. Souza Santos, and S.P. Toledo. 2000. "Standard Transition Aluminas. Electron Microscopy Studies." Materials Research 3(4): 104–114.
- [8.] Sathyaseelan, Balaraman, Iruson Baskaran, and Kandasamy Sivakumar. 2013. "Phase Transition Behavior of Nanocrystalline Al<sup>2</sup>O<sup>3</sup> Powders." Soft Nanoscience Letters 3(4): 69–74.

### **Publications**

### **Special Workshop**

- [1.] "Ion and Neutron Irradiation of Nuclear Materials," A GEMMA Project Workshop November 2021.
- [2.] "The Key Enabling Role of Ductile Amorphous Oxide Coatings for GIV and Fusion Nuclear Power Plant," IAEA 2022.

#### **Oral Presentation**

- [3.] "The Key Enabling Role of Ductile Amorphous Oxide Coatings for the Commercialization of Thermonuclear Fusion Power," OMC Conference 2021, ISBN: 978-88946678-0-6.
- [4.] "Ductile Amorphous Coatings: A Key Technology for Heavy Liquid Metal Fast Reactors," NuMat 2022.
- [5.] "The Key Role of Heavy Ion Irradiation in the Development of Ductile Amorphous Oxide Barrier Coatings for Next-Generation Nuclear Power Plants," CAARI 2022.

Distributed Partnership at a Glance			
NSUF Institution	Facilities and Capabilities		
Argonne National Laboratory:	The Intermediate Voltage Electron Microscopy (IVEM) — Tandem Facility		
Collaborators			
Italian Institute of Technology	Davide Loiacono (Team Member), Boris Paladino (Team Member),		
Argonne National Laboratory	Wei-Ying Chen (Team Member), Peter M. Baldo (Team Member		
Degrees Granted			
Politecnico di Milano / Italian Institute of Technology	Boris Paladino, Ph.D. Davide Loiacono, Ph.D.		

### Evolution of Ga<sub>2</sub>O<sub>3</sub> Native Point Defects, Donors, and Acceptors with Neutron Irradiation

Leonard J. Brillson - The Ohio State University - brillson.1@osu.edu

he team proposed to use nanometer-scale, depthresolved cathodoluminescence spectroscopy (DRCLS), surface photovoltage spectroscopy (SPS), and Hall-effect measurements to study the dependence of free carrier density n, mobility  $\mu$ , donor density N<sub>D</sub>, and acceptor density N<sub>A</sub> on neutron-irradiation dose and subsequent forming gas (FG) anneals. With this combination of techniques and processing, the team aimed to understand the effect of neutron irradiation on the creation of native point defects such as gallium vacancies V<sub>Ga</sub>, oxygen vacancies V<sub>O</sub>, Ga interstitials G<sub>al</sub>, and related complexes.

### **Experimental or Technical Approach**

The team studied the optical, electrostatic, and electrical properties of neutron-irradiated  $Ga_2O_3$  over a wide range of irradiation doses, starting at orders-of-magnitude lower dosages. The team proposed four neutron irradiations—1 x10<sup>14</sup> neutrons cm<sup>-2</sup>, 1 x1015 neutrons cm<sup>-2</sup>, 1 x10<sup>16</sup> neutrons cm<sup>-2</sup>, and 1 x10<sup>17</sup> neutrons cm<sup>-2</sup>—which required four weeks to complete but only 11 s, 110 s, 18.3 minutes, and 1.5 hours, respectively, of active irradiation per sample for four.

At each stage of irradiation dosage, the team used DRCLS and SPS to measure optical-luminescence transitions involving defect states with energy-level positions in the  $Ga_2O_3$  band gap. Likewise, the team was able to measure carrier density n, mobility  $\mu$ ,  $N_D$ , and  $N_A$  of the irradiated samples at each dosage level and with FG anneals.

#### Results

Edge-fed growth Ga<sub>2</sub>O<sub>3</sub> samples were all irradiated uniformly with ~1 x 10<sup>15</sup> neutrons per cm<sup>2</sup>. All four irradiated wafers exhibited dominant depth-dependent defect emissions at 3.07 and 3.53 eV, commonly associated with gallium and oxygen vacancies, respectively. The relative amplitudes of these features and the lower-intensity features at 1.6 and 1.73 eV vary with wafer and spots within wafers. The 1.73 eV peak appears to vary with the 3.07 dominant peak, unlike the 1.6 eV peak, which may be a secondorder replica. These features vary with excitation depth and increase at the shallowest depth. Finally, a relatively weak 2.4-2.56 eV shoulder appears in one wafer spectrum, particularly near the free surface. This feature may be associated with Ga vacancy complexes according to some theoretical predictions.

### **Discussion/Conclusion**

Overall, numerous defect features appear and distribute nonuniformly between wafers and across individual wafers after 1 x 10<sup>15</sup> neutrons per cm<sup>2</sup>. These nonuniformities are new and may be related to the high neutron fluence. Additional experiments will be needed to identify the physical nature of the 1.73 eV and 2.4-3.56 eV emissions using, as an example, FG anneals, which are known to passivate Ga vacancies.

### **Publications**

[1.] Gao, Hantian, et al. 2021.

"Depth-Resolved Cathodoluminescence and Surface Photovoltage Spectroscopies of Gallium Vacancies in β-Ga<sub>2</sub>O<sub>3</sub> with Neutron Irradiation and Forming Gas Anneals." Journal of Vacuum Science & Technology B 39: 052205. https://doi.org/10.1116/6.0001240.

Distributed Partnership at a Glance			
NSUF Institution	Facilities and Capabilities		
The Ohio State University	The Ohio State University Nuclear Research Laboratory		
Collaborators			
The Ohio State University	Leonard J. Brillson, Ph.D		
Degrees Granted			
The Ohio State University	Hantain "George" Gao Ph.D.		

### Heavy Ion Irradiation and Characterization of Light-Refractory, Body-Centered Cubic, High-Entropy Alloys

Michael Moorehead - Idaho National Laboratory - michael.moorehead@inl.gov



hile body-centered cubic (BCC) steels are known to incur less void swelling than their face-centered cubic counterparts under similar irradiation conditions, few studies have examined the performance of BCC high-entropy alloys (HEAs) under irradiation at temperatures relevant for promoting void swelling (i.e., approximately half the melting point). The purpose of this research project is to experimentally examine the role of chemical complexity on the irradiation response of singlephase, BCC, light-refractory HEAs, which are relevant for advanced nuclear reactor applications.

### Experimental or Technical Approach

Four increasingly complex light refractory HEAs were examined,  $Cr_{33}Mn_{33}V_{33}$ ,  $Cr_{31}Mn_{31}Ti_7V_{31}$ ,  $Al_{15}Cr_{20}Mn_{20}Ti_{10}V_{35}$ , and  $Al_{15}Co_4Cr_{20}Mn_{20}Ti_6V_{35}$ , and are all in atomic percent. Alloy composition selection was informed by calculation of phase diagrams (CALPHAD) modeling, via PanDat and the PanHEA database, which were used to search for HEAs that exhibited a single-phase microstructure at elevated temperatures and contained large amounts of Al, Cr, and Ti to form

passivating oxides and remove interstitial impurities from solid solution. These impurities are known to embrittle refractory metals. Alloys were produced via arc melting and subjected to a 1200°C homogenization heat treatment to ensure each started with a single-phase, BCC microstructure as confirmed by X-ray diffraction. Samples of each alloy were irradiated at the Wisconsin Ion Beam Laboratory at 500°C using 4-MeV, defocused V2+ ions to a maximumdose of 100 dpa in the damage plateau region. PIE was performed at the University of Wisconsin-Madison Characterization Laboratory for Irradiated Materials facility, where a focused ion beam was used to prepare sample lamellae for TEM using an FEI Technai TF-30 TEM instrument. TEM analysis was used for assessing the presence of radiation-induced precipitation and void swelling and for examining the dislocation loops and networks generated under irradiation.

#### Results

After 100 dpa at 500°C, TEM analysis revealed radiation-induced precipitation in the damage region in three out of four studied alloys. Based on CALPHAD predictions, the radiation-induced precipitates in Cr<sub>33</sub>Mn<sub>33</sub>V<sub>33</sub> are likely a Mn-rich

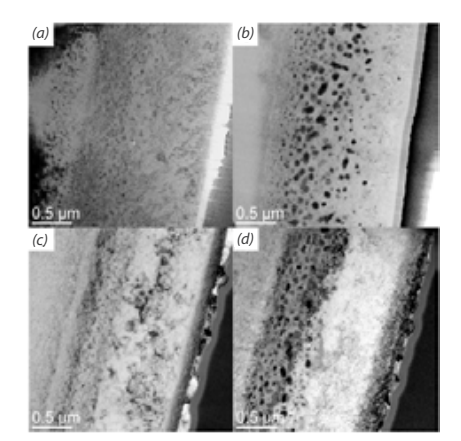


Figure 1: Bright-field TEM micrographs of (a)  $Cr_{33}Mn_{33}V_{3y}$  (b)  $Cr_{31}Mn_{31}Ti7V_{3y}$  (c)  $AI_{15}Cr_{20}Mn_{20}TI_{10}V_{3y}$  and (d)  $AI_{15}Co_4Cr_{20}Mn_{20}TI_6V_{35}$  after irradiation with 4-MeV V2+ ions at 500°C to 100 dpa in the damage plateau region.

sigma phase near the damage peak, while Cr<sub>31</sub>Mn<sub>31</sub>Ti<sub>7</sub>V<sub>31</sub> appears to have formed a Ti-rich Laves phase, which is pervasive over the entire damage region. Al<sub>15</sub>Co<sub>4</sub>Cr<sub>20</sub>Mn<sub>20</sub>Ti<sub>6</sub>V<sub>35</sub>, with both Co and Ti additions, likely formed a combination of Co-rich, ordered, B2 precipitates and formed Ti-rich Laves phase precipitates. Of the light refractory HEAs irradiated to 100 dpa, only the least complex alloy (Cr<sub>33</sub>Mn<sub>33</sub>V<sub>33</sub>) showed evidence of minor void swelling, which lends credence to the idea that increased chemical complexity leads to improved tolerance to irradiation damage. However, further irradiations at different temperatures and higher doses would be needed to compare the swelling curves and the incubation doses for the more-complex alloys before a causal determination can be made.

### **Discussion/Conclusion**

While sparce voids were observed in one of the light-refractory HEAs studied, most alloys formed radiation-induced precipitates after irradiation. Being that V is only a minor constituent in the radiation-induced precipitate compositions, it is suspected that the formation of these precipitates is caused by

the irradiation-enhanced diffusion kinetics rather than changes in chemistry caused directly by the injection of V ions. This suggests that only Al<sub>15</sub>Cr<sub>20</sub>Mn<sub>20</sub>Ti<sub>10</sub>V<sub>35</sub> could be expected to remain microstructurally stable after prolonged exposure in a reactor environment.

Distributed Partnership at a Glance			
NSUF Institution	Facilities and Capabilities		
University of Wisconsin-Madison	Characterization Laboratory for Irradiated Materials		
Collaborators			
University of Wisconsin-Madison	Adrien Couet (Co-Principal Investigator), Hongliang Zhang (Team Member)		
Fermi National Accelerator Laboratory	Frederique Pellemoine (Team Member), Kavin Ammigan (Team Member)		

## Understand the Fission Products Behavior in UCO Fuel Kernels of Safety Tested Advanced Gas-Cooled Reactor TRISO Fuel Particles by Using Titan Themis 200 with ChemiSTEM Capability

Yong Yang -University of Florida - yongyang@ufl.edu



n support of the Fuel Qualification program, the project aims to acquire knowledge of irradiated microstructure and physical and chemical states of fission products in irradiated TRISO fuel particle kernels.

### **Experimental or Technical Approach**

Microstructure characterizations, elemental analysis, and phase identification were conducted using a Titan Themis 200 scanning transmission electron microscope. Characterizations included STEM, bright-field (BF), high-angle annual dark field imaging, energy-dispersive X-ray spectroscopy (EDS) elemental mapping, and selected-area electron diffraction.

#### **Results**

The studies yielded several results shown in Figure 1. The team found that the irradiated-fuel kernel microstructure consists of UO<sub>2</sub> and UC(O) phases. Additionally, fission products of Zr, Ru, and Tc tend to concentrate in the UC(O) phase or precipitate to form U(Mo)C<sub>2</sub> or URuC<sub>2</sub> phases when the concentrations of Ru and Tc exceed their solubility limits in UC(O) phase. A third observation the team made is that Nb is prone to forming Nb oxides at the peripherals of pores or cracks.

#### **Discussion/Conclusion**

The knowledge of chemical states of fission products can help to estimate the oxygen potential more accurately in the irradiated particle fuels. The observation of Pd immobilized in U<sub>2</sub>RU<sub>2</sub>C<sub>2</sub> phase can potentially provide a mechanistic explanation for the superior irradiation performance of UCO TRISO fuel particles compared to UO<sub>2</sub> particle fuel.

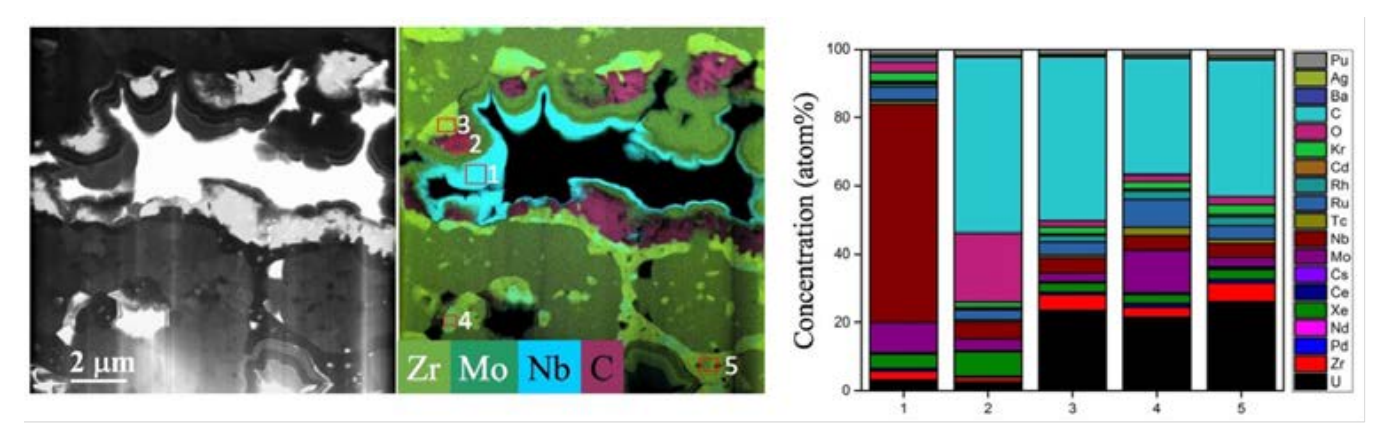


Figure 1. Characterization of irradiated AGR-2 fuel kernel half center: (a) BF TEM image, (b) Zr, Mo, Nb, and C elemental mapping, and (c) compositional analysis from automated optical inspection labeled on (b).

### References

[1.] Fu, Zhenyu, et al. 2021.

"Microstructural and MicroChemical Evolutions in
Irradiated UCO Fuel Kernels
of AGR-1 and AGR-2 TRISO
Fuel Particles." Journal of
Physics: Conference Series
2048: 012006. https://
doi.org/10.1088/17426596/2048/1/012006.

Distributed Partnership at a Glance			
NSUF Institution	Facilities and Capabilities		
Idaho National Laboratory	Irradiated Materials Characterization Laboratory		
Collaborators			
Idaho National Laboratory	Isabella van Rooyen (Co-Principal Investigator), Lingfeng He (Co-Principal Investigator)		
University of Florida	Zhenyu Fu (Team Member)		
Degrees Granted			
University of Florida	Zhenyu Fu, Ph.D.		

### IVEM Investigation of Defect Evolution in FCC Compositionally Complex Alloys under Dual-Beam Heavy-Ion Irradiation

Calvin Parkin - University of Wisconsin-Madison - cparkin@wisc.edu, caparki@sandia.gov



onventional nuclear structural alloys degrade severely after hundreds of displacements per atom, inadequately meeting the needs of next-generation fast reactors and triggering an investigation of compositionally complex alloys (CCA). Preliminary studies have shown that these alloys exhibit excellent mechanical properties and irradiation tolerance at hightemperature, promoting their candidacy for cladding and duct applications [1-20]. To investigate the fundamental mechanisms underlying the radiation resistance of compositionally complex base matrices, in situ dual-beam irradiations were performed on Cr<sub>18</sub>Fe<sub>27</sub>Mn<sub>27</sub>Ni<sub>28</sub> and Cr<sub>15</sub>Fe<sub>35</sub>Mn<sub>15</sub>Ni<sub>35</sub> at two elevated temperatures. Bubble populations were characterized at various dpa steps and compared to less compositionally complex reference materials.

### **Experimental or Technical Approach**

Electropolished discs of  $Cr_{18}Fe_{27}Mn_{27}Ni_{28}$  and  $Cr_{15}Fe_{35}Mn_{15}Ni_{35}$ were irradiated in situ using the 300 keV Hitachi-9000 TEM at the IVEM-Tandem facility at Argonne National Laboratory (ANL) using a 1 MeV Kr<sup>2+</sup> and 16 keV He<sup>+</sup> dual-ion beam with a He/dpa ratio of 0.75%/ dpa. Alloy selection, fabrication, preparation, precharacterization, and stopping range of ions in matter (SRIM) software inputs are detailed in references [11] and [3]. Pure Ni and a single-phase Fe<sub>56</sub>Ni<sub>44</sub> binary alloy were used for reference against the two FCC CCAs. Two irradiation temperatures were selected: 500°C and 600°C. All irradiations but one were performed up to 7 dpa, as estimated by IVEM-developed correlations between counts measured by a Faraday cup and both SRIM and Iradina calculations for the dpa through a 100 nm-thick specimen [21, 22]. The 500°C Ni irradiation was performed to 1 dpa with a He/dpa ratio of 1%/dpa, as detailed in reference [23]. Dpa profiles for combined and individual ion species and He implantation are

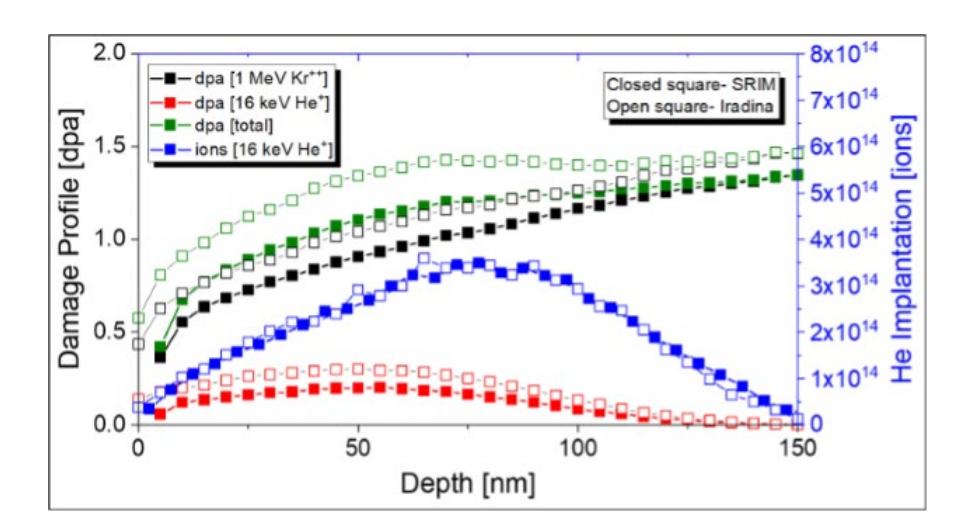


Figure 1.  $Kr^{2+}$  and  $He^+$  dpa and implantation profile for  $Cr_{18}Fe_{27}Mn_{27}Ni_{28}$  generated by SRIM. Average of 1 dpa within first 100 nm.  $Kr^{2+}$  ions are high enough in energy to pass through the samples with minimal implantation.

shown in Figure 1. Bubble formation was confirmed using underfocused and overfocused conditions. Bubble diameters were measured using ImageJ software and used to calculate swelling levels. Lamellae thicknesses were measured by direct electron method (K2 camera) and a slit width of 15 eV.

#### **Results**

The bubble population for all materials at both temperatures at their final dpa is shown in Figure 2. The average bubble diameters, bubble number densities, and swelling levels are plotted in Figure 3. For each material, bubbles nucleate with higher density and with a smaller size at 500°C relative to 600°C, and the average diameter of bubbles remains higher at 600°C up to the maximum dpa. Due to the high density of bubble nucleation at 500°C, the swelling

in Cr<sub>18</sub>Fe<sub>27</sub>Mn<sub>27</sub>Ni<sub>28</sub> is slightly higher than at 600°C despite the limited bubble size (<2 nm diameter), which contrasts with the pure Ni and Fe<sub>56</sub>Ni<sub>44</sub> binary alloy that exhibit significantly higher swelling at 600°C. The swelling levels in Cr<sub>15</sub>Fe<sub>35</sub>Mn<sub>15</sub>Ni<sub>35</sub> at both temperatures are comparable; this indicates that although mobility is increased at 600°C, similar quantities of vacancies and interstitials can arrive at both bubbles and other sinks. Between the two temperatures, the bubble densities in Cr<sub>15</sub>Fe<sub>35</sub>Mn<sub>15</sub>Ni<sub>35</sub> are closer together than were seen in Cr<sub>18</sub>Fe<sub>27</sub>Mn<sub>27</sub>Ni<sub>28</sub>, which demonstrates a reduced temperature effect on the mobility of vacancies and He atoms. Swelling levels in the two CCAs are consistently lower than the less compositionally complex materials.

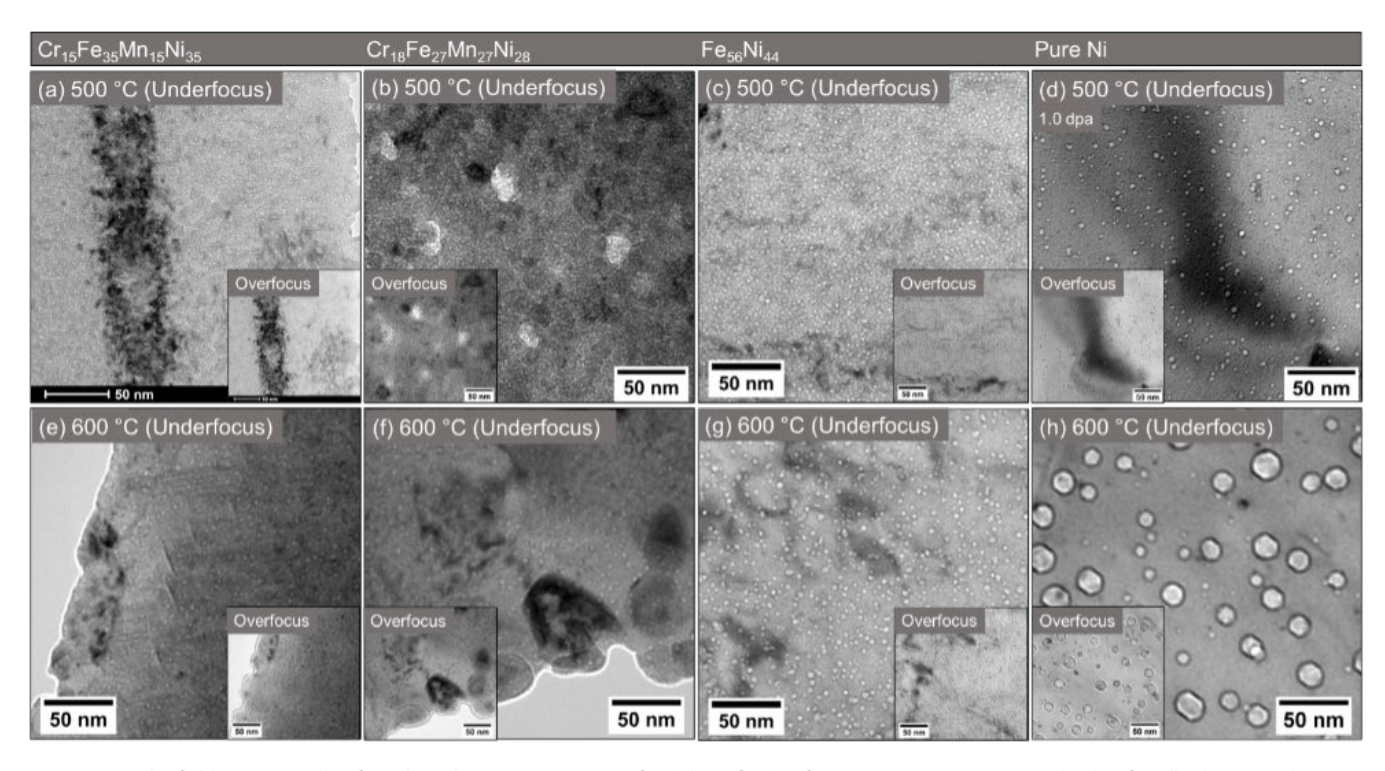


Figure 2. Bright-field micrographs of irradiated microstructures at final dpa of 1 dpa for pure Ni at  $500^{\circ}$ C [23] and 7 dpa for all other samples.

### **Discussion/Conclusion**

Under favorable void-swelling conditions (i.e., dual-beam and high-temperature), bubbles nucleated in all irradiated materials. Under single-beam irradiation at 50 K, it was shown that  $Cr_{18}Fe_{27}Mn_{27}Ni_{28}$  and  $Cr_{15}Fe_{35}Mn_{15}Ni_{35}$  experienced a lower primary point defect production term than pure Ni and E90, a FeNiCr ternary alloy [11]. This reduction

likely slowed bubble growth in CCAs compared to pure Ni and Fe<sub>56</sub>Ni<sub>44</sub>. Reference [23] proposed that vacancies generated in pure Ni under dual-beam conditions trap He atoms, leading to uniform nucleation of bubbles. In CCAs, the more localized and denser bubble nucleation is attributed to a distorted lattice, further trapping vacancies and He atoms.

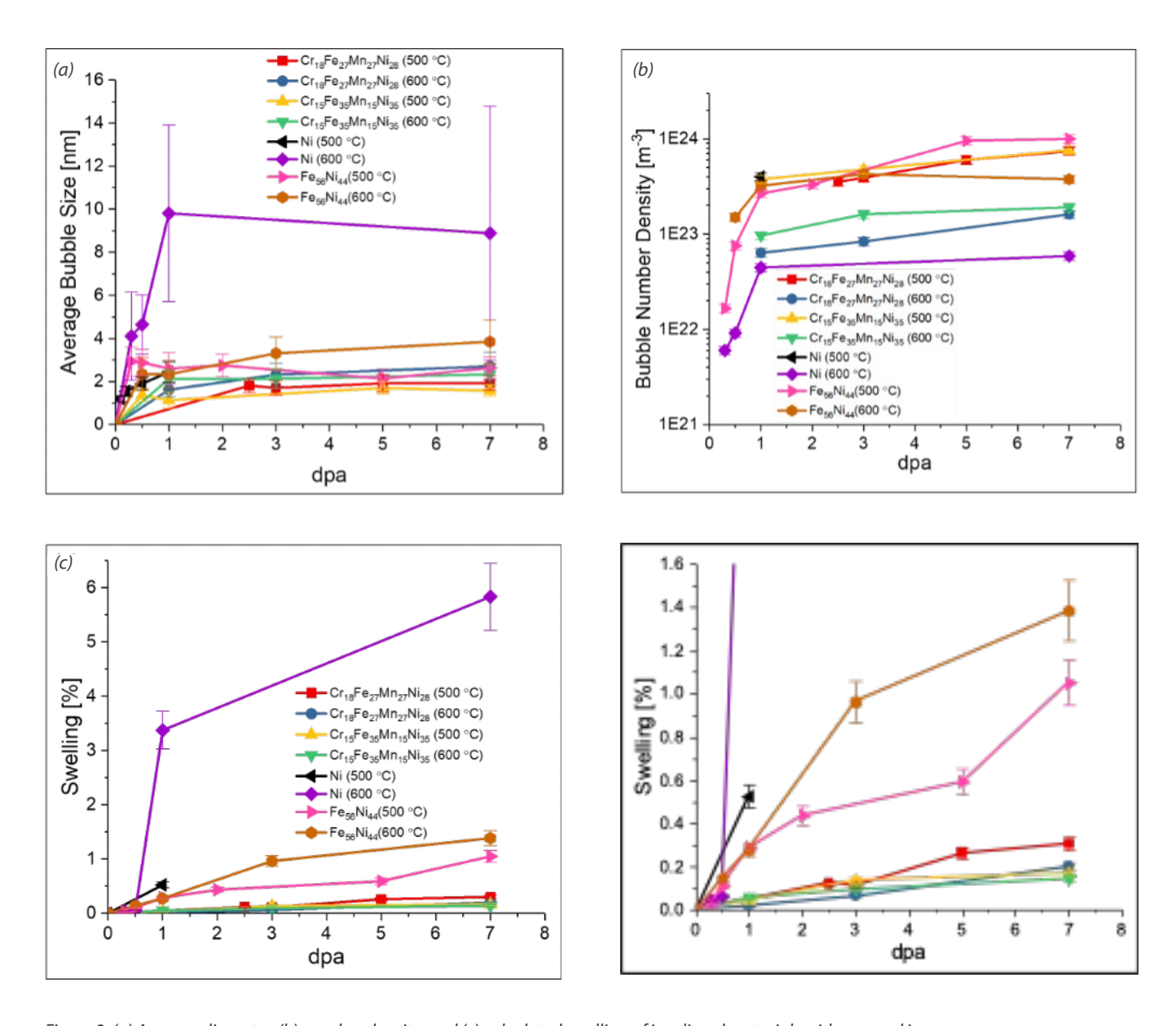


Figure 3. (a) Average diameter, (b) number density, and (c) calculated swelling of irradiated materials with zoomed in swelling axis on the right for clarity.

#### References

- [1.] Miracle, D., and O. Senkov. 2017. "A Critical Review of High Entropy Alloys and Related Concepts." Acta Materialia 122: 448–511.
- [2.] Kumar, N.A.P.K., et al. 2016.

  "Microstructural Stability

  And Mechanical Behavior of

  FeNiMnCr High Entropy Alloy

  under Ion Irradiation." Acta

  Materialia 113: 230–244.
- [3.] Parkin, C., et al. 2022. "Phase Stability, Mechanical Properties, and Ion Irradiation Effects in Face-Centered Cubic FeCrMnNi Compositionally Complex Solid-Solution Alloys at High Temperatures." Journal of Nuclear Materials 565: 153733.
- [4.] Egami, T., et al. 2013. "Irradiation Resistance of Multicomponent Alloys." Metallurgical and Materials Transactions A 45: 180–183.
- [5.] Jin, K., et al. 2016. "Effects of Compositional Complexity on the lon-Irradiation Induced Swelling and Hardening in Ni-Containing Equiatomic Alloys." Scripta Materialia 119: 65–70.

- [6.] .Yang, T., et al. 2018. "Irradiation Responses and Defect Behavior of Single-Phase Concentrated Solid Solution Alloys." Journal of Materials Research 33 (19): 3077–3091.
- [7.] Lu, C., et al. 2016. "Enhancing Radiation Tolerance by Controlling Defect Mobility and Migration Pathways in Multicomponent Single-Phase Alloys." Nature Communications 7: 13564.
- [8.] Lu, C., et al. 2017. "Radiation-Induced Segregation on Defect Clusters in Single-Phase Concentrated Solid-Solution Alloys, Acta Materialia 127: 98–107.
- [9.] Jin, K., and H. Bei. 2018. "Single-Phase Concentrated Solid-Solution Alloys: Bridging Intrinsic Transport Properties and Irradiation Resistance." Frontiers in Materials 5 (26).
- [10.] Shi, S., et al. 2018. "Evolution of Ion Damage at 773K in Ni- Containing Concentrated Solid-Solution Alloys." Journal of Nuclear Materials 501: 132–142.

- [11.] Parkin, C., et al. 2020. "In Situ Microstructural Evolution in Face-Centered and Body-Centered Cubic Complex Concentrated Solid-Solution Alloys under Heavy Ion Irradiation." Acta Materialia 198: 85–99.
- [12.] Chen, W.-Y., et al. 2018.

  "Irradiation Effects in High
  Entropy Alloys and 316H
  Stainless Steel at 300°C."

  Journal of Nuclear Materials
  510: 421–430.
- [13.] Li, C., et al. 2019. "Neutron Irradiation Response of a Co-Free High Entropy Alloy." Journal of Nuclear Materials 527: 151838.
- [14.] Egami, T., et al. 2015. "Local Electronic Effects and Irradiation Resistance in High-Entropy Alloys." The Journal of The Minerals, Metals & Materials Society 67 (10): 2345–2349.
- [15.] Körmann, F., et al. 2017. "Phonon Broadening in High Entropy Alloys." Computational Materials Science 3.

- [16.] Zhang, Y., et al. 2016. "Influence of Chemical Disorder on Energy Dissipation and Defect Evolution in Advanced Alloys."

  Journal of Materials Research 31 (16): 2363–2375.
- [17.] Zhao, S., et al. 2019. "Frenkel Defect Recombination in Ni and Ni-Containing Concentrated Solid-Solution Alloys." Acta Materialia 173: 184–194.
- [18.] Caro, M., et al. 2015. "Lattice Thermal Conductivity of Multi-Component Alloys." Journal of Alloys and Compounds 648: 408–413.
- [19.] Béland, L., Y. Osetsky, and R. Stoller. 2016. "The Effect of Alloying Nickel with Iron on the Supersonic Ballistic Stage of High Energy Displacement Cascades." Acta Materialia 116: 136–142.

- [20.] Zhang, Y., et al. 2015. "Influence of Chemical Disorder on Energy Dissipation and Defect Evolution in Concentrated Solid Solution Alloys." Nature Communications 6.
- [21.] Stoller, R.E., et al. 2013. "On the Use of SRIM for Computing Radiation Damage Exposure."
- [22.] Crocombette, J., and C.V.
  Wambeke, "Quick Calculation
  of Damage for Ion Irradiation:
  Implementation in Iradina
  and Comparisons to SRIM."
  EPJ Nuclear Sci. Technol. 5 (7)
  (2019).
- [23.] Chen, W.Y., and M. Li. 2022.

  "Helium Bubble Formation in
  Nickel under In-Situ Krypton
  and Helium Ions Dual-Beam
  Irradiation." Journal of Nuclear
  Materials 558: 153342.

#### **Publications**

[1.] Parkin, C., et al. (under review).,
"Microstructural Evolution of
Compositionally Complex
Solid-Solution Alloys under
Dual-Beam Irradiation.", Acta
Materialia.

Distributed Partnership at a Glance			
NSUF Institution	Facilities and Capabilities		
Argonne National Laboratory	Intermediate Voltage Electron Microscopy — Tandem Facility		
Collaborators			
Argonne National Laboratory	Wei-Ying Chen (Co-Principal Investigator)		
University of Wisconsin-Madison	Adrien Couet (Co-Principal Investigator)		
Degrees Granted			
University of Wisconsin-Madison	Calvin Parkin, Ph.D.		

# NSUF LIST OF ACRONYMS

3D	Three-dimensional
AML	Activated Materials Laboratory
APS	Advanced Photon Source
BCC	Body-centered cubic
BF	Bright field
CA	
CAES	Center for Advanced Energy Studies
CAO	Calcium oxide
CCA	Compositionally complex alloys
CINR	Consolidated Innovative Nuclear Research
CLIM	Characterization Laboratory for Irradiated Materials
COVID-19	
CVI	Chemical vapor infiltration
CVD	Chemical vapor deposition
DCFI	Drift-corrected frame integration
DNS	Double-notch shear
DISECT	Disc Irradiation for Separate Effects Testing
DOE	Department of Energy
DOE-NE	Department of Energy, Office of Nuclear Energy
DRCLS	Depth-resolved cathodoluminescence spectroscopy
EDS	Energy-dispersive X-ray spectroscopy
EMPAD	Electron microscope pixel array detector
EPP0	End-plug push-out

FCC
FGForming ga
FIBFocused ion bear
HEA High entropy allo
HFIR High Flux Isotope Reacto
HPCHigh-performance computing
HSiC Hybrid silicon carbid
iDPCIntegrated differential phase contras
IMETIrradiated Materials Examination and Testing Facilit
INLIdaho National Laborator
LAMDALow Activation Materials Design and Analysis Laborator
LBB Long Beamline Buildin
LFALaser flash analysi
LWRLight water reacto
MASTODON Multi-hazard Analysis for STOchasti time-DOmaiN phenomen
MOOSEMultiphysics Object Oriented Simulation Environmen
NFMLNuclear Fuels and Materials Librar
NSUFNuclear Science User Facilitie
OFFERReurOpean platForm For accEssing nucleaR R&d facilitie
ORNLOak Ridge National Laborator
PIPrincipal investigato
PIF Post-irradiation evamination

PLDPulsed laser deposi	tion
RICRadiation-induced crystalliza	tion
RTE Rapid Turnaround Experim	ient
SAED Selected-area electron diffrac	tion
SAM-2SAMple (library experimen	t)-2
SEMScanning electron microsc	ope
SiC Silicon carl	oide
SRIMStopping and range of ions in ma	itter
SPSSurface photovoltage spectroso	ору
STEM Scanning transmission electron microsc	ope
TEPTransient eutectic ph	ıase
TEMTransmission electron microsc	ope
TREAT Transient Test Reactor Test Fac	ility
TRISOTristructural isotr	opic
WIBLWisconsin Ion Beam Labora	tory
XCTX-ray computed tomogra	phy
XRDX-ray diffrac	tion



## INDEX

### **Partner Institutions:**

Argonne National Laboratory (ANL): 2, 14,15, 18, 34, 35, 36, 38, 46, 47, 48, 49, 83, 90, 95

Argonne National Laboratory: *Advanced Photon Source (APS)*, 34, 36

Argonne National Laboratory: Activated Materials Laboratory (AML), 3, 34, 36

Argonne National Laboratory: The Intermediate Voltage Electron Microscopy (IVEM) – Tandem Facility, 46, 47, 48, 49, 83, 90, 95

Belgian Center for Nuclear Research (SCK/CEN):

Belgian Reactor 2, Laboratory for High and Medium Activity, 9

Brookhaven National Laboratory (BNL): 14, 18, 46, 48

Brookhaven National Laboratory: National Synchrotron Light Source II (NSLS-II), 46, 48 Center for Advanced Energy Studies (CAES): 14, 17, 20, 21, 44, 46, 47, 48, 49

Idaho National Laboratory (INL): 11, 14, 15, 17, 20, 22, 24, 41, 42, 43, 44, 45, 46, 47, 48, 49, 68, 73, 74, 79, 86, 89

Idaho National Laboratory: *Advanced Test Reactor (ATR)*, 10, 17, 30, 31, 48

Idaho National Laboratory: *High-Performance Computing* (HPC), 3, 6, 22, 23, 27, 28, 29, 41, 64

Idaho National Laboratory: Irradiated Materials Characterization Laboratory (IMCL), 44, 45, 46, 47, 48, 49, 50, 73, 74, 79, 89

Idaho National Laboratory: *Materials & Fuels Complex (MFC)*, 17, 26, 99

Lawrence Livermore National Laboratory (LLNL): 14

Los Alamos National Laboratory (LANL): 14, 15, 48

Massachusetts Institute of Technology (MIT): 14, 44

North Carolina State University (NCSU): 14, 15, 49

Oak Ridge National Laboratory (ORNL): 14, 15, 18, 46, 47, 48, 53, 66, 67

Oak Ridge National Laboratory: *High Flux Isotope Reactor (HFIR)*, 52, 53, 55, 56, 58, 63, 66, 67

Oak Ridge National Laboratory: Irradiated Materials Examination and Testing Facility (IMET) Hot Cells, 56

Oak Ridge National Laboratory: Low Activation Materials Design and Analysis Laboratory (LAMDA), 46, 47, 47, 55, 56, 67

The Ohio State University (OSU): 14, 15, 46, 48, 84, 85



The Ohio State University: *The Ohio* State University Nuclear Research Laboratory, 85

Pacific Northwest National Laboratory (PNNL): 18, 48

Pacific Northwest National Laboratory: *Materials Science & Technology Laboratory (MSTL)*, 48

Pacific Northwest National Laboratory: *Radiochemical Processing Laboratory (RPL)*, 22

Penn State University: 44, 57

Purdue University: 14, 15, 44, 46, 47

Sandia National Laboratories (SNL): 14

Texas A&M University (TAMU): 14, 17, 44, 46, 47, 73, 74, 79

Texas A&M University: Accelerator Laboratory, 44, 46, 47, 74, 79

University of California, Berkeley (UCB): 14

University of Florida (UF): 14, 15, 47, 88, 89

University of Michigan (UM): 14, 15, 46, 47, 48

University of Michigan: *Michigan Ion Beam Laboratory (MIBL)*, 47, 48

University of Michigan: Michigan Center for Materials Characterization, 47

University of Wisconsin, Madison: 14, 15, 46, 74, 79, 86, 87, 90, 95

University of Wisconsin: 46

University of Wisconsin: Characterization Laboratory for Irradiated Materials, 86, 87

Westinghouse: 14, 73

Westinghouse: *Churchill Laboratory Services*, 73



### **Collaborators**

Bachhav, Mukesh Idaho National Laboratory 73

Baldo, Peter Argonne National Laboratory 83

Brillson, Leonard The Ohio State University 84, 85

Chen, Wei-Ying Argonne National Laboratory 83, 95

Couet, Adrien University of Wisconsin-Madison 46, 79, 87, 95

Deck, Christian General Atomics 52,

Di Fonzo, Fabio Italian Institute of Technology 80

Fu, Zhenyu University of Florida 89

Garner, Frank Texas A&M University
73

Gonderman, Sean General Atomics 67

He, Lingfeng Idaho National Laboratory 48, 79, 89

Ickes, Michael Westinghouse Electric Company 73

Jiang, Wen Idaho National Laboratory 73 Kombaiah, Boopathy Idaho National Laboratory 73

Koyanagi, Takaaki Oak Ridge National Laboratory 66, 67

Loiacono, Davide Italian Institute of Technology 83

Moorehead, Michael Idaho National Laboratory 86

Paladino, Boris Italian Institute of Technology 83

Parkin, Calvin University of Wisconsin-Madison 74, 78, 79, 90, 94, 95

Pellemoine, Frederique Fermi National Accelerator Laboratory 87

Petrie, Christian Oak Ridge National Laboratory 66, 67

Porter, Douglas Idaho National Laboratory 73

Shatoff, Herb General Atomics 67

Sun, Cheng Idaho National Laboratory 68, 73, 100

van Rooyen, Isabella Idaho National Laboratory 89

Yang, Yong University of Florida 88

Zhang, Hongliang University of Wisconsin-Madison 87





